ACS OMEGA

http://pubs.acs.org/journal/acsodf

Article

Pharmacological Basis for Antispasmodic, Bronchodilator, and Antidiarrheal Potential of *Dryopteris ramosa* (Hope) C. via In Vitro, In Vivo, and In Silico Studies

Iram Iqbal, Fatima Saqib,* Muhammad Farhaj Latif, Hamna Shahzad, Lorena Dima,* Bayan Sajer, Rosana Manea, Ciprian Pojala, and Radu Necula

Cite This: *ACS Omega* 2023, 8, 26982−27001

Read Online

ACCESS | Metrics & More | Article Recommendations

ABSTRACT: *Background: Dryopteris ramosa* is used as an old treatment for several diseases. *D. ramose* fronds are eaten to treat gastrointestinal (GIT) issues and as an antibiotic. However, there is a dearth of literature justifying its traditional use. *Aims and objectives*: the current work used biological and molecular docking studies to support traditional usage and elucidate *D. ramosa*'s multitarget mechanism. *Materials and methods:* Bioactive compounds were docked in silico. Force displacement transducers coupled with a power lab data gathering system examined the effects of compounds on rabbit jejunum, trachea, and aorta tissues. Albino mice and rats were used for in vivo studies. *Results:* Bioactive compounds interacted with inflammation, asthma, and diarrhea genes, according to in silico studies. *D. ramosa* crude extract (Dr.Cr) calmed impulsive contractions and K+ (80 mM)-provoked contractions in the jejunum and tracheal tissue dose-dependently, showing the presence of the Ca++ channel-blocking (CCB) effect, further verified by the rightward parallel shift of CRCs equivalent to verapamil. Polarity-based fractionation showed spasmolytic activity in Dr.DCM and muscarinic receptors mediated spasmogenic activity in the Dr.Aq fraction. Dr.Cr vasoconstricted the aortic preparation, which was totally blocked by an angiotensin II receptor antagonist. This suggests that Dr. Cr's contractile effect is mediated through angiotensin receptors. In rats and mice, it showed anti-inflammatory and antidiarrheal action. *Conclusion:* This study supports the traditional medicinal uses of *D. ramosa* against GIT disorders and may be an important therapeutic agent in the future.

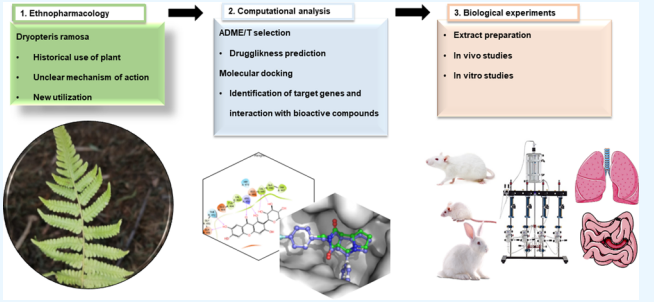

1. INTRODUCTION

Since the beginning of their evolutionary history, humans have had discrete pharmacological knowledge of the medicinal effects of plants, leaving traces in prehistoric and subsequent cultural heritage.[1] Ethnopharmacology is the scientific study of conventional medical procedures and how many cultures use plants, animals, and minerals for therapeutic purposes. But there have also been a number of disputes around this topic including cultural appropriation and violation of intellectual property rights of native people, as there are instances where pharmaceutical companies have patented traditional practices without the consent of indigenous communities. These debates show how important it is for ethnopharmacology to take ethical concerns and cultural sensitivity seriously in order to uphold and value indigenous knowledge and practices.[2] Besides this, recently, the transition from conventional ethnopharmacology to drug discovery has been facilitated by the introduction of specialized extraction techniques including sophisticated new methodologies such as high-performance liquid chromatography (HPLC), liquid chromatography-mass spectrometry (LC-MS), gas chromatography-mass spectrometry (GC-MS), chemoinformatic techniques, the advancement of isolation and characterization techniques, and the rise in computing power including molecular docking and gene target prediction of compounds.[1] A lot has been accomplished recently in the rapidly developing discipline of ethnopharmacology. Using cutting-edge methods like metabolomics and high-throughput screening, scientists are discovering new molecules in traditional medicinal plants. These substances have the potential to be turned into novel treatments and medications.[3] The validity of the effectiveness and safety of conventional medicines has been greatly aided by ethnopharmacology. Clinical trials are being carried out by researchers to examine the efficacy of conventional treatments

Received: March 21, 2023
Accepted: June 21, 2023
Published: July 20, 2023

for a variety of illnesses, such as cancer, diabetes, and infectious disorders, as we already know a number of drugs including taxol, vinca alkaloids (vinblastine, vincristine), quinine, and artemisinin, which are isolated from plants.[1] People are more interested in using medicinal plants as a result of their conviction that plant extracts are more effective, readily accessible, inexpensive, and have few adverse effects than other options.[3] Ayurvedic medicines and Chinese ancient medicine have grown in fame as complementary therapies for serious ailments in recent years.[4] Ma huang, ginseng, ginkgo, P. zizyphi, magnolia, bupleurum, and Huang qin are typical Chinese herbs employed to treat asthma,[5,6] while in the Unani medical system commonly used formulation is Qurs Sartan Kafoori (for the treatment of chronic bronchitis, cough, and tuberculosis).[7]

Due to its rich biodiversity and diverse climate zones, Pakistan is home to a diverse array of medicinal plants. In the North, it has the Himalayan range, the Hindu Kush range, and the Karakoram range.[8,9] The Himalayas is regarded as a botanical treasure trove.[8] The Himalayan people are well-versed in the use of medicinal herbs for traditional reasons. These herbs are employed not only as healing agents for fever, chest, and intestinal disorders but also as a key raw material in the production of traditional and modern medications.[10] Since ancient times, ferns have been employed as a remedy for a variety of human ailments, including bruises, burns, bleeding, colds, diarrhea, constipation, gastric ulcers, and many more.[11]

Dryopteris ramosa, also known as kunji or pakha, is a medicinally important plant native to the Himalayan region that grows in wet and shaded areas at high altitudes.[10,12] It is used as a vegetable against ulceration in the gastrointestinal tract, for constipation,[13−15] and as an aphrodisiac,[13] provides strength to the body,[14] and acts as a vulnerable diuretic and stomachic, having antibacterial potential and febrifuge.[16] The juice from the plant is used to relieve stomach aches.[17]As it acts as an astringent, so in addition to its therapeutic purposes, it also has some cosmetic benefits.[16]

Ferns have survived since the Paleozoic era; it is hypothesized that they have some distinctively useful secondary metabolites in comparison to other plant species. Studies have discovered many useful phytochemicals from the ferns, those counting different alkaloids, flavonoids, phenols, steroids, triterpenoids, amino acids, and fatty acids, thus providing an indication for the medicinal significance of the plant.[18] *D. ramosa* has presented marked antibacterial, antifungal, enzyme inhibition,[12] and antioxidant activities.[12,19]

2. METHODOLOGY

2.1. Extract Preparation. *D. ramosa* Linn. (http://www.theplantlist.org, accessed 04-07-2021) was collected from Haripur, KPK during July−Aug 2021 and identified by the assistance of expert taxonomist Prof Dr. Muhammad Zafar, Quaid-e-Azam University, Islamabad, and voucher specimen # 131415 was deposited in the herbarium of Pakistan, Quaid-e-Azam University, Islamabad. The plant was washed and air-dried at ambient temperature for about 2 weeks and ground into a coarse powder. 1 kg of the powder was then added to a solution of 70:30 ethanol/water in an amber glass flask for maceration with periodic shaking for 7 days. To remove herbal pieces, this soaked substance was first filtered using a muslin cloth, and the liquid thus obtained was later filtered by filter paper, and a similar method was used for the second and third time maceration. Later on, all collected filtrates were combined and concentrated on a Rota evaporator (BUCHI) at 37 ± 2 °C. A layer of the semisolid substance (Dr.Cr) with a dark brown color and honey-like consistency is produced with a % yield of 15% approx. The resulting extract was kept in an amber-colored airtight bottle in a cool, dry location (a refrigerator set to −4 °C) for further studies. Fractionation was accomplished by combining 20 g of Dr.Cr with 100 mL of distilled water (DW) and 100 mL of dichloromethane (DCM), resulting in one DCM layer and another aqueous layer. Both layers were separated out and dried, giving fractions of Dr.Dcm and Dr.Aq, respectively.[20,21]

2.2. Chemicals. Experiments were conducted using compounds of approx. 99.9% purity. Calcium chloride ($CaCl_2$), sodium chloride (NaCl), glucose ($C_6H_{12}O_6$), potassium chloride (KCl), sodium bicarbonate ($NaHCO_3$), potassium dihydrogen phosphate (KH_2PO_4), magnesium sulfate ($MgSO_4$), magnesium chloride ($MgCl_2$), sodium dihydrogen phosphate (NaH_2Po_4), and ethyl alcohol (C_2H_5OH) were provided by Merck, Deemastadt, (Germany). Acetylene chloride, ethylenediaminetetraacetic acid (EDTA), atropine sulfate, aspirin, carbachol (CCh), phenylephrine (PE), acetylcholine (Ach), cyproheptadine, pyrilamine, verapamil HCl were bought from Sigma Chemical Co., St. Louis, MO. Ammonium hydroxide and sodium hydroxide were provided by BDH Laboratory Supplies, England.

2.3. Animal Housing. For the experimental purpose, albino rabbits (♀/♂, weight: 1.5−2.0 kg), Sprague Dawley rats (♀/♂, weight: 150−250 g), and mice (♀/♂, weight: 20−30 g) were obtained from Animal House, Faculty of Pharmacy, Bahauddin Zakariya University, Multan. Animals were retained under controlled environmental conditions at a temperature of 23 ± 3 °C and 30−70% relative humidity, followed by a light and dark cycle with standard food and ad libitum water. Animals were given unrestrained water access but were denied meals the night before the trial. Rabbits were killed after a blow to the neck, whereas mice and rats were sacrificed via cervical dislocation. All permitted ethical rules specified by "The Institute of Laboratory Animal Resources, Commission on Life Sciences" (NRC,1996) were trailed in the whole research.[22]

2.4. Qualitative Phytochemical Detection. Exploratory phytochemical screening of *D. ramosa* crude ethanolic extract (Dr.Cr) was performed to identify secondary metabolites of the plant like cardiac glycosides, flavonoids, saponins, tannins, alkaloids, phenols, and steroids.

2.5. In Silico Approaches. *2.5.1. ADMET Profile and Drug-Likeness.* The previously identified bioactive compounds of *D. ramosa* (gallic acid, quercetin, caffeic acid, vanillic acid, cinnamic acid,[23] iriflophenon glycoside,[24] mangiferin, isomangiferin,[19] and verapamil) were evaluated for absorption, distribution, metabolism, excretion, and toxicity (ADMET) in the Quickprop module of Maestro (Schrodinger Suite 2015), SWISS ADME (http://www.swissadme.ch/, accessed on: May 28, 2022)[25] and PkCSM (http://biosig.unimelb.edu.au/pkcsm/prediction, accessed on 28 May 2022)[26] to evaluate ADMET and drug-likeness parameters. Several rules, such as (1) Lipinski's rule of 5, (2) Ghose rule, (3) Veber's rule, (4) Egan's rule, and (5) Muegge's rule, were applied to the target compounds via SWISS ADME to confirm their drug-like properties and to recognize the count of debased parameters. The ADMET properties like water solubility, topological polar surface area, molar refractivity, $CaCO_2$ cell permeability, volume of distribution, intestinal absorption, unbound fraction,

https://doi.org/10.1021/acsomega.3c01907
ACS Omega 2023, 8, 26982−27001

hepatotoxicity, total renal clearance, and ability to inhibit the P-glycoprotein were also calculated using pkCSM.

2.5.2. Molecular Docking. The previously reported method of Sirous et al.[27] was used to perform molecular docking studies for protein and bioactive compounds.

2.5.2.1. Ligand Preparation. The PubChem database (https://pubchem.ncbi.nlm.nih.gov, accessed on May 28, 2022) was employed to retrieve two-dimensional (2D) structures of already reported bioactive compounds from *D. ramosa*, and these ligands were modified in the LigPrep module of Maestro (Schrodinger Suite 2018, Schrödinger, Inc. NY) for the ionization, minimization, and optimization of ligands. The Epik tool of this module was used to produce the ionization state of ligands at cellular pH (7.4 ± 0.5), and the OPLS3e force field was applied using the module for minimization as well as optimization of these ligand structures that produce the minimal energy conformers of ligands.

2.5.2.2. Protein Preparation. Maximum-resolution protein X-ray structures for molecular docking were retrieved using the Protein Databank (RCSB PDB) (https://www.rcsb.org., accessed on May 28, 2022). These structures were put through the Maestro (Schrodinger Suite 2018, Schrödinger, Inc., New York) Protein Preparation Wizard to add H-atoms to the structure of the protein, remove extra water molecules from the solvents, assign bond orders, create disulfide bridges, fill in the absent side chains, and generate the protonation condition using the Epik tool for protein assemblies for ligands at the cellular level pH (7.4 ± 0.5). Following refining, PROPKA was used at pH 7.0 to improve the protein structures. Using the OPLS3e force field, we carried out restrained minimization for energy and geometry optimization of the protein structure.

2.5.2.3. Receptor Grid Generation. The Receptor Grid Generation module of Maestro defined the active regions of protein structures for molecular docking (Schrodinger Suite 2018). With the use of some already bound protein ligands and existing literature, a cubic grid block for each protein was created. The grid box's dimensions were changed to be 16 Å long. The potential of the receptor's nonpolar components was reduced to 1.0 Å on the van der Waals radius of nonpolar protein atoms with a partial atomic charge cutoff of 0.25 Å.

2.5.2.4. Molecular Docking. The premade ligand structures and protein structures were put via Maestro's Ligand Docking (Glide) module's extra precision (XP) mode (Schrodinger Suite 2018), utilizing a grid file for the receptor that had already been created. A 0.80 Å van der Waals radii scaling factor was changed with a partial charge cutoff of 0.15 Å. Using the VSGB solvation model and the OPLS3e force field, the Prime MM-GBSA module was utilized to analyze the docking results and identify the binding dynamics of ligand molecules with the target protein structure.

2.5.2.5. Inhibition Constant (K_i). The following equation was used for the calculation of the inhibition constant by using the binding free energy of a ligand previously produced by Prime MM-GBSA.

$$dG = -RT(\ln K_i)$$

or

$$K_i = \exp(-dG/RT)$$

where dG = binding free energy of the ligand, R = gas constant (cal mol^{-1} K^{-1}), R = gas constant (cal mol^{-1} K^{-1}), and T = normal ambient temperature (298 K).

2.6. In Vitro Assays. Isolated tissue responses in physiological conditions were noted by Bio science isometric and isotonic force displacement transducers attached to the Power lab data acquisition system (AD Instruments, Bella Vista, NSW, Australia), displaying results on a computer having lab chart software (version 6) installed. The effect of the test substance was measured as the percentage change in the response of tissue recorded after the administration of test doses.[28,29]

2.6.1. Preparation of Isolated Jejunum. Rabbits were sacrificed to obtain the jejunum. Mesenteries were removed from the tissue, and jejunal segments of 2−3 cm lengths were prepared and suspended in priorly filled 15 mL of tissue organ baths having carbogen (5% CO_2 and 95% O_2) bubbling through Tyrode's solution having NaCl (136.9 mM), $NaHCO_3$ (11.90 mM), $MgCl_2$ (1.05 mM), KCl (2.68 mM), glucose (5.55 mM), $CaCl_2$ (1.8 mM), and NaH_2PO_4 (0.42 mM) and maintained at 37 °C. All tissues were permitted to equilibrate for around 30 min, before being stabilized with a 3 min interval of Ach (1 μM) to get a persistent tissue response prior to the inclusion of any drug solution or plant extract. Before starting the experiment, the isolated tissue organ bath fluid was replaced with fresh Tyrode solution, and spontaneous rhythmical contractions were noted prior to testing the drug. The possible spasmolytic or spasmogenic response of Dr.Cr was studied on equilibrated jejunal preparation by cumulative addition of different doses of Dr.Cr. A dose−response curve was created, and the response was reported as a percentage of the control contractions. For determination of CCB activity, 80 mM KCl was used to precontract the jejunum.[30,31]

To further illustrate the Ca++ channel antagonistic action, isolated rabbit jejunum tissues were stabilized in regular Tyrode solutions, that solution was subsequently replaced with calcium-free Tyrode solution containing 0.1 mM EDTA (chelating agent), for around 30 min. This solution was then replaced with Ca++-free and K+-rich Tyrode solution having NaCl (91.0 mM), $NaHCO_3$ (11.89 mM), $C_6H_{12}O_6$ (5.6 mM), KCl (50.1 mM), Na_2HPO_4 (0.43 mM), EDTA (0.12 mM), and $MgCl_2$ (2.0 mM) for about 30 min to get stability. The control of concentration−response curves (CRCs) of Ca++ was created by applying Ca++ concentration in a cumulative way. A gradual increase in the contraction of jejunal tissue indicates the dependency of the contractile response of smooth muscles on extracellular calcium.[28,31]

After two cycles, superimposable curves were attained, and tissues were then washed and given time to stabilize in the presence of various dose concentrations of Dr.Cr, and CRCs were recreated after incubation times of 50 ± 10 min and compared with control curves.[31]

2.6.2. Preparation of Isolated Trachea. The trachea was divided into 2−3 mm rings (2−3 cartilaginous rings) after being dissected. The tracheal rings were cut longitudinally on the side opposing smooth muscle, creating a strip having smooth muscles sandwiched between cartilaginous sides of the strip. Following that, the tissues were fixed in an isolated tissue organ bath having carbogen (5% CO_2 and 95% O_2) bubbling through Krebs solution having NaCl (118.2 mM), $NaHCO_3$ (25.0 mM), $CaCl_2$ (2.5 mM), KCl (4.7 mM), $MgSO_4$ (1.2 mM), and glucose (11.7 mM) and maintained at 37 °C. A preload stress of 1 g was given to tissues, and the tissues were permitted to equilibrate for 50 ± 10 min prior to any experiment.

https://doi.org/10.1021/acsomega.3c01907
ACS Omega 2023, 8, 26982−27001

Table 1. ADMET Profiling of Bioactive Compounds of *Dryopteris ramosa*[a]

parameters	quercetin	verapamil	caffeic acid	vanillic acid	cinnamic acid	iriflophenon glycoside	gallic acid	mangiferin	isomangiferin
mol_MW	302.24	454.608	180.16	168.149	148.161	408.361	170.121	422.345	422.345
QPlogPoct	18.568	19.073	12.439	10.056	8.672	27.834	13.33	30.016	29.413
QPlogPw	14.428	6.393	9.878	8.113	5.688	22.572	12.015	25.851	25.62
QPlogPo/w	0.367	3.856	0.545	1.042	1.897	−0.841	−0.579	−1.702	−1.811
QPlogS	−2.909	−5.766	−1.293	−1.393	−1.616	−2.491	−0.68	−2.505	−2.252
QPlogHERG	−5.109	−6.792	−2.169	−1.601	−2.348	−5.16	−1.401	−5.006	−4.429
QPPCaco	18.199	848.556	22.354	77.585	206.809	5.182	10.235	3.618	3.058
QPlogBB	−2.419	−0.444	−1.546	−0.883	−0.548	−3.439	−1.652	−3.467	−3.329
QPPMDCK	6.511	458.292	10.343	39.698	114.551	1.675	4.446	1.136	0.947
QPlogKp	−5.544	−2.642	−4.499	−3.787	−2.54	−6.18	−5.468	−6.774	−7.032
QPlogKhsa	−0.343	0.847	−0.804	−0.747	−0.518	−0.789	−0.987	−0.899	−0.851
CNS permeability	−2	1	−2	−1	−1	−2	−2	−2	−2
percent human oral absorption	51.649	100	54.287	66.869	79.497	21.85	41.634	1.055	0
GIT absorption	high	high	high	high	high	low	high	low	low
intestinal absorption (human)	77.207	92.836	69.407	78.152	94.833	46.248	43.374	46.135	48.512
bioavailability score	0.55	0.55	0.56	0.85	0.85	0.55	0.56	0.17	0.17
BBB permeant	no	yes	no	no	yes	no	no	no	no
CYP1A2 antagonist	yes	no	no	no	no	no	no	no	no
CYP2C19 antagonist	no	no	no	no	no	no	no	no	no
CYP2C9 antagonist	no	no	no	no	no	no	no	no	no
CYP2D6 antagonist	yes	yes	no	no	no	no	no	no	no
CYP3A4 antagonist	yes	yes	no	no	no	no	yes	no	no
P-glycoprotein substrate	yes	yes	no	no	no	yes	no	yes	yes
P-glycoprotein I blocker	no	yes	no	no	no	no	no	no	no
P-glycoprotein II blocker	no	yes	no	no	no	no	no	no	no
Lipinski violations	0	0	0	0	0	1	0	2	2
Ghose violations	0	2	0	0	2	1	2	1	1
Veber violations	0	1	0	0	0	1	0	1	1
Egan violations	0	0	0	0	0	1	0	1	1
Muegge violations	0	0	1	1	1	2	1	3	3

[a]MW: molecular weights of the molecules in Dalton, i.e.,130.0−500.0; QPlogPo/w: the forecast lipophilicity partition coefficient of octanol/water, ranging from 2 to 6.5; QPlogS: aqueous solubility predicted: −6.5 to 0.5; QPlogHERG: IC50 for HERG K+ channel blockade predicted > 5; QPPCaco: foreseeable apparent Caco-2 cell, a model for the gut−blood barrier, with weak permeability if 25 and large permeability if >500; QPlogBB: brain/blood partition coefficient predicted, −3 to 1.2; QPPMDCK: blood−brain barrier nonactive transport predicted by apparent MDCK cell permeability in nm/sec with 25 bad and >500 fantastic predictions; QPlogKp: skin permeability predicted, −8.0 to −1.0 cm/s; QPlogKhsa: anticipated serum albumin binding of human, −1.5 to 1.5; and CNS permeability: greater than −2 able to penetrate.

High K (KCl, 80 mM) and carbachol (1 μM) were utilized in order to achieve a persistent agonistic response for the purpose of determining the broncho-relaxant action of Dr.Cr. A sustained reaction is attained after 45 min, at which point the extract was applied cumulatively to attain a concentration-dependent inhibitory response of the extract. Isometric tissue responses were captured using Bio science transducers.[31]

2.6.3. Preparation of Isolated Aorta. To examine the impact of the plant extract on vascular resistance, the descending thoracic portion of the aorta was cut into 2−3 mm broad rings, placed in isolated tissue organ baths individually, and given 50 ± 10 min to equilibrate. At the beginning of the experiment and throughout, a preload stress of 2 g was applied. Each tissue organ bath had carbogen (5% CO_2 and 95% O_2) bubbling through Krebs solution having NaCl (118.2 mM), $NaHCO_3$ (25.0 mM), $CaCl_2$ (2.5 mM), KCl (4.7 mM), $MgSO_4$ (1.2 mM), and glucose (11.7 mM) and was kept at a temperature of 37 °C. To clarify any potential vasorelaxant or vasoconstrictor effects, Dr.Cr was added cumulatively to a baseline resting state.[32] Prazocin, losartan, and cyproheptadine were used as pretreatments on isolated aortic rings in order to clarify the mechanism of contraction.[33]

2.7. In Vivo Activity. *2.7.1. Anti-Inflammatory Activity.* The previously described carrageenan-induced rat paw edema assay was used to test Dr.Cr for its possible anti-inflammatory effect, after minor adjustments.[34] 20 Wistar albino rats (♀, ♂) weighing between 180 and 220 g were divided into four groups, i.e., Group I: control group (0.9% saline), Group II: drug group (aspirin 0.01 g/kg), and Groups III and IV: test groups of Dr.Cr doses (0.1 and 0.2 g/kg, respectively). Edema was induced by inoculating 1% carrageenan into the sub-planter area of the right hind paw after 55 ± 5 min of dose administration (IP) of Dr.Cr, and the extent of the edema was measured up to 4 h later using a plethysmometer (UGO Basile, Italy). Results were expressed as the percentage inhibition of edema.

2.7.2. Castor Oil-Induced Diarrhea. Twenty mice of either gender (♀, ♂) were randomly divided into four groups having five animals in each group to test the antidiarrheal effects of the Dr.Cr extract. Before the experiment, all of the groups were kept in separate cages with free access to water; however, food was withheld for the night prior to testing. Group I labeled as the negative control group was orally given 0.9% saline (NS) at a dose of 10 mL/kg. Loperamide (10 mg/kg) was given orally to Group II, which was designated as the positive control

https://doi.org/10.1021/acsomega.3c01907
ACS Omega 2023, 8, 26982−27001

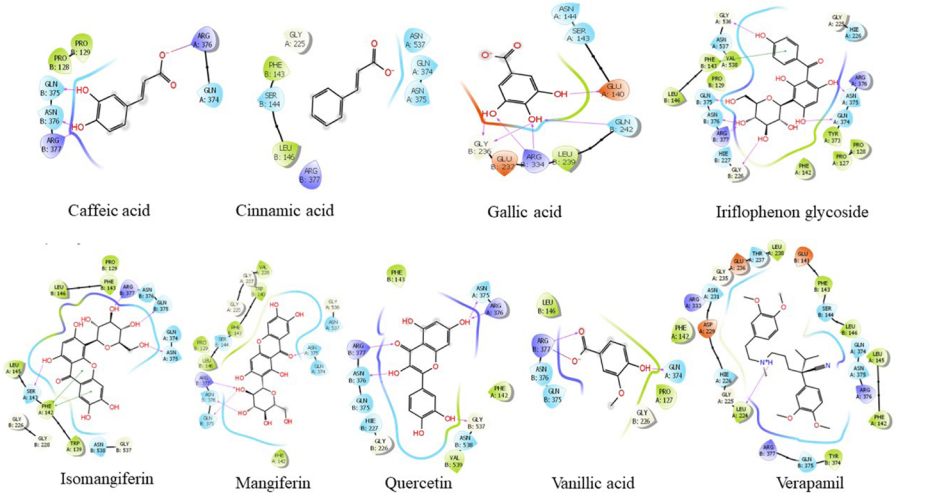

A: Human Cyclooxygenase-2 (COX2-PDB:5IkQ)

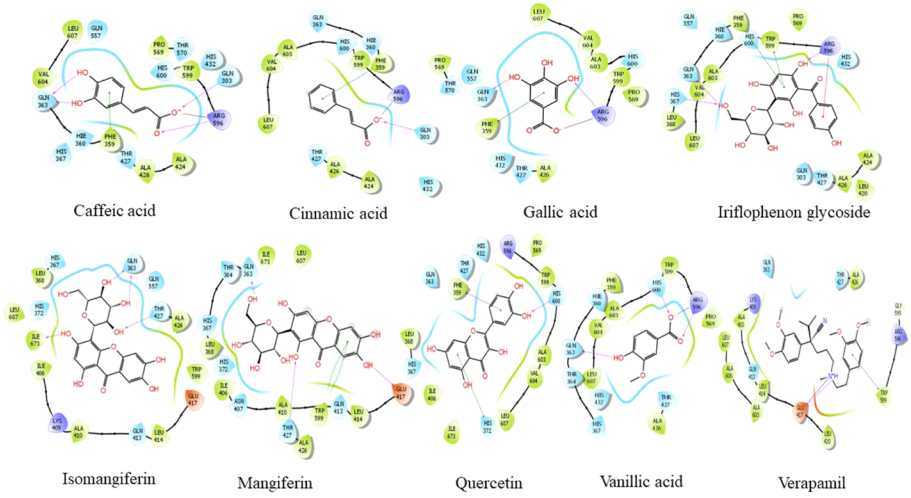

B: Arachidonate¬-5-Lipoxygenase (ALOX5, PDB:6n2w)

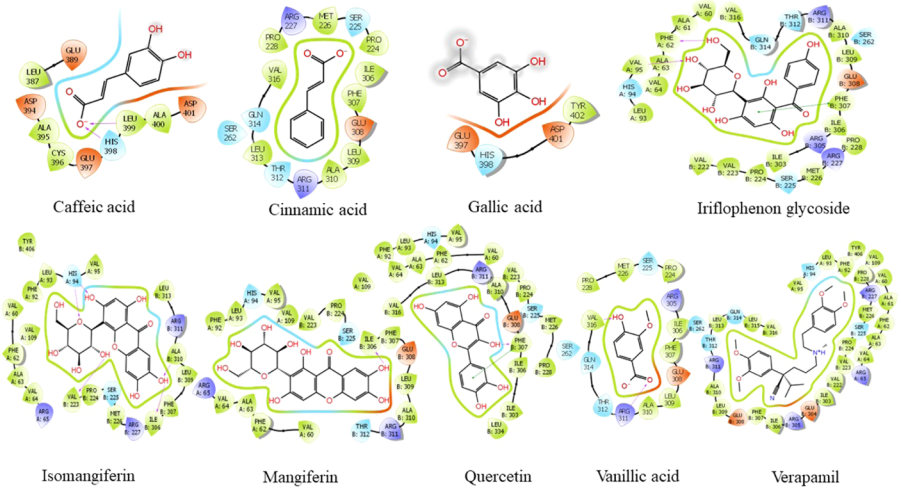

C: Voltage gated calcium ion channel beta2a (VGCC,PDB:1T0J)

Figure 1. continued

https://doi.org/10.1021/acsomega.3c01907
ACS Omega 2023, 8, 26982−27001

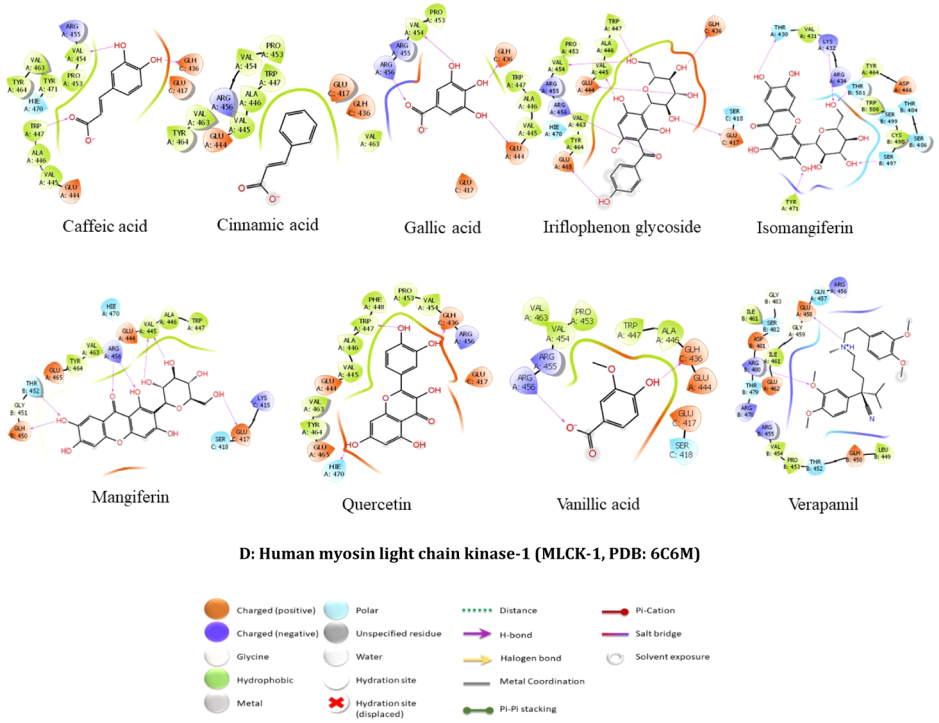

Figure 1. Two-dimensional protein/ligand interaction between bioactive compounds (caffeic acid, cinnamic acid, gallic acid, mangiferin, quercetin, vanillic acid, and verapamil) and proteins: (A) human cyclooxygenase-2 (COX2-PDB:5IkQ), (B) arachidonate-5-lipoxygenase (ALOX5, PDB:6n2w), (C) voltage-gated calcium ion channel β2a (VGCC, PDB:1T0J), and (D) human myosin light chain kinase-1 (MLCK-1, PDB: 6C6M).

group. Groups III and IV were given Dr.Cr doses of 0.2 and 0.4 g/kg, respectively. 30 min after the administration of treatment, all groups were orally administered 10 mL/kg castor oil to induce diarrhea and monitored for wet diarrheal spots for up to 4 h.[28] The mean amount of feces for each group was determined and the outcomes were presented as %age inhibition.

$$[(D_{cn} - D_t)/D_{cn}] \times 100$$

where D_{cn} is the mean defecation of the control group and D_t is the mean defecation of the test group.

2.8. Statistical Analysis. All of the results are expressed as mean ± (S.E.M). "GraphPad Prism (GraphPad, San Diego, California: http://www.graphpad.com)" was utilized to obtain the median effective concentrations (EC_{50} value) with a 95% (CI). In the instance of the in vivo study, statistical analysis was one-way ANOVA and two-way ANOVA, and it was further trailed by Dunnett's test, where a probability of ($p < 0.05$)* was deemed significant statistically.[35]

3. RESULTS AND DISCUSSION

Natural medicine has seen a significant rise in popularity over the last two decades.[36] Ethnopharmacological methods offer hints in the search for bioactive substances.[24] *Dryopteris ramosa* has many traditional uses including its use in GIT disorders and also as a febrifuge. Therefore, this study was designed to validate the potential mechanisms of *D. ramosa* in digestive and respiratory systems by an integrated strategy of molecular docking of *D. ramosa* bioactive compounds and its validation through different in vitro and in vivo experimental models.

3.1. Pilot Phytochemical Screening. Preliminary phytochemical analysis of ethanolic extract (Dr.Cr) showed flavonoids, glycosides, saponins, phenols, tannins, and steroids amid secondary bioactive metabolites of the plant. Flavonoids have been shown to have antispasmodic and calcium channel-blocking properties.[37,38]

3.2. In Silico Studies. *3.2.1. ADMET Analysis.* A literature review shows that several bioactive compounds have been extracted from *D. ramosa* including gallic acid, quercetin, caffeic acid, vanillic acid, cinnamic acid, iriflophenon glycoside, mangiferin, and isomangiferin.[19,23,24] These compounds were subjected to an ADMET analysis utilizing the Schrödinger QikProp module,[39] SWISS ADME, and PkCSM (Table 1). The aqueous solubility, octanol/water partition coefficient, and a number of other physical characteristics may all be predicted. Cell permeability, the brain/blood partition coefficient, QPlogKhsa to forecast binding affinity to serum albumin of humans, and QPlogHERG to measure HERG K+ channel blockade and human oral absorption percentage were determined.

3.2.2. Molecular Docking. Docking seeks to appropriately assess the strength of binding by accurately predicting a ligand's shape inside the confines of a binding pocket.[40] The bioactive compounds iriflophenon glycoside, isomangiferin, mangiferin, quercetin, gallic acid, caffeic acid, vanillic acid, cinnamic acid, and verapamil were docked with selected proteins, human cyclooxygenase-2 (COX2-PDB: 5IkQ), arachidonate-5-lipoxygenase (ALOX5, PDB: 6n2w), voltage-gated calcium ion channel β2a (VGCC, PDB: 1T0J), and human myosin light chain kinase-1 (MLCK-1, PDB: 6C6M), to check their affinity with binding sites of these proteins for the possible mechanism of action. According to earlier research, quercetin and caffeic acid may have antispasmodic effects,[41,42] and quercetin is reported to be a regulator of the tone of GIT,[43] thus leading to the presence of antispasmodic as well as antidiarrheal effects of the plant. Our results showed

https://doi.org/10.1021/acsomega.3c01907
ACS Omega 2023, 8, 26982−27001

Table 2. Docking Score and Binding Energies of Bioactive Compounds with Human Cyclooxygenase-2, Arachidonate-5-Lipoxygenase, Voltage-Gated Calcium Ion Channel β2a, and Human Myosin Light Chain Kinase-1[a]

compounds	docking score	glide energy	dG bind	log pK_i	dG Coulomb	dG covalent	dG H-bond	dG lipo	dG solv GB	dG vdW	H-bond	other bonds
Human Cyclooxygenase-2 (COX2-PDB: 5IkQ)												
iriflophenon glycoside	−9.77	−47.43	−37.8	−13.19	−33.69	15.91	−4.35	−12.54	44.69	−44.92	conventional H-bond: Val538 (2.77 Å), Arg377 (2.15 Å), Gly226 (2.24 Å), Asn376 (1.69 Å), Gln375 (1.72 Å), Gln374 (1.97 Å), Asn375 (1.83 Å), Gly536 (1.92 Å), carbon H-bond: Pro129 (2.75 Å), Arg377 (2.61 Å), Asn376 (2.67 Å), Asn376 (3.04 Å), π-donor hydrogen bond: Asn375 (2.90 Å)	π-cation; π-donor hydrogen bond: Arg376 (4.18 Å)
isomangiferin	−8.85	−50.25	−38.57	−13.52	−34.55	4.97	−3.05	−12.18	53.78	−44.74	conventional H-bond: Arg377 (2.87 Å), Arg377 (2.08 Å), Gln375 (2.81 Å), Gln375 (1.82 Å), Asn375 (1.98 Å), Ser143 (2.08 Å), carbon H-bond:Gly226 (2.63 Å), (2.88 Å), Gln375 (2.59 Å)	π-cation: Arg376 (4.97 Å), $\pi-\pi$ T-shaped: Phe142 (4.63 Å), π-alkyl: Leu145 (5.25 Å)
mangiferin	−8.03	−48.09	−26.53	−8.29	−23.06	3.41	−3.29	−13.24	55.81	−43.45	conventional H-bond: Val228 (2.66 Å), Asn375 (1.76 Å), Arg377 (2.05 Å), Arg377 (3.00 Å), Gln375 (2.46 Å), Asn376 (1.82 Å), (1.93 Å), carbon H-bond: Gln374 (2.46 Å), Gln375 (2.79 Å)	
quercetin	−8	−45.98	−44.83	−16.24	−25.9	2.58	−3.39	−7.5	31.3	−36.8	conventional H-bond: Arg376 (2.46 Å), Arg376 (2.93 Å), Arg377 (2.26 Å), Val539 (2.81 Å), Asn376 (1.99 Å), (1.82 Å), Asn375 (2.08 Å), Gly537 (1.82 Å), π-donor hydrogen bond: Asn376 (2.80 Å)	
gallic acid	−6.88	−31.09	−9.38	−0.84	−53.63	5.2	−4.3	−5.38	64.83	−15.34	conventional H-bond: Gln242 (2.04 Å), Gln242 (2.57 Å), Arg334 (2.02 Å), Arg334 (1.86 Å), Gly236 (1.85 Å), Gly236 (1.75 Å), Glu140 (1.95 Å), carbon H-bond: Ser143 (2.71 Å), Asn144 (2.91 Å), Leu239 (2.68 Å), π-lone pair: Glu237 (2.90 Å)	
caffeic acid	−6.05	−26.07	−14.17	−2.92	−49.11	7.63	−3.97	−6.03	58.65	−19.9	conventional H-bond: Arg376 (2.13 Å), Arg377 (2.03 Å), Gln375 (1.73 Å), Asn376 (1.70 Å)	electrostatic attractive charge: Arg376 (3.38 Å)
vanillic acid	−5.46	−24.62	−14.42	−3.03	−49.45	2.98	−3.01	−5.97	64.34	−21.31	conventional H-bond: Arg377 (2.11 Å), Arg377 (2.11 Å), Gln374 (1.91 Å), carbon H-bond: Gly226 (2.97 Å)	electrostatic attractive charge: Arg377 (3.47 Å)
verapamil	−4.31	−49.04	−27.11	−8.54	53.87	6.01	−1.45	−22.1	−2.17	−58.64	conventional H-bond: Arg376 (2.78 Å), Leu224 (2.08 Å), carbon H-bond: Ser144 (2.32 Å), Gln375 (2.76 Å), Tyr374 (2.75 Å), Gln374 (2.48 Å), Tyr374 (2.56 Å), Gly235 (2.57 Å), Glu236 (2.79 Å), Asp229 (2.68 Å), Glu141 (2.73 Å), Glu141 (2.70 Å)	alkyl: Pro129 (5.04 Å), Pro127 (4.94 Å), Leu238 (4.61 Å), π-alkyl: Phe142 (4.87 Å), Phe143 (5.18 Å)
cinnamic acid	−2.15	−16.3	0.79	3.57	−24.01	0.29	−0.24	−9.29	59.7	−24.34	conventional H-bond: Asn375 (2.64 Å), carbon H-bond: Gln374 (2.88 Å)	$\pi-\pi$ T-shaped: Phe143 (4.50 Å)

https://doi.org/10.1021/acsomega.3c01907
ACS Omega 2023, 8, 26982−27001

Table 2. continued

compounds	docking score	glide energy	dG bind	log pK_i	dG Coulomb	dG covalent	dG H-bond	dG lipo	dG solv GB	dG vdW	H-bond	other bonds
Arachidonate-5-lipoxygenase (ALOX5, PDB: 6n2w)												
isomangiferin	−8.55	−49.99	−47.84	−17.55	−35.88	3.77	−2.92	−13.67	41.82	−39.95	conventional H-bond: Thr427 (2.27 Å), Gln363 (1.79 Å), Gln363 (1.65 Å), Ile673 (2.20 Å), (1.87 Å), carbon H-bond: Leu368 (2.61 Å), His372 (2.79 Å)	
mangiferin	−8.03	−41.78	−30.3	−9.93	−19.03	5.51	−3.04	−11.85	36.28	−34.25	conventional H-bond: His367 (2.19 Å), Thr427 (1.80 Å), Thr427 (2.99 Å), Gln363 (1.88 Å), (1.56 Å), (1.84 Å), Glu417 (2.05 Å), carbon H-bond: (2.57 Å), carbon H-bond: Gln363 (3.07 Å)	$\pi-\sigma$: Trp599 (2.50 Å), $\pi-\pi$ T-shaped: Trp599 (5.89 Å), Trp599 (4.96 Å)
iriflophenon glycoside	−7.03	−37.37	−32.17	−10.74	−29.05	6.29	−2.64	−13.17	43.47	−33.02	conventional H-bond: His367 (2.09 Å), Arg596 (2.77 Å), Gln363 (1.76 Å), (1.63 Å), (1.79 Å), carbon H-bond: Thr427 (3.06 Å), His432 (2.45 Å), Gln363 (2.77 Å), Gln363 (2.99 Å)	π-cation: Arg596 (2.79 Å), $\pi-\pi$ T-shaped: Phe359 (5.33 Å), Trp599 (5.41 Å), π-alkyl: Ala603 (5.43 Å), Ala426 (3.67 Å)
caffeic acid	−5.19	−25.45	−16.09	−3.76	48.9	4.99	−2.7	−10.6	−27.91	−26.83	conventional H-bond: Gln303 (2.19 Å), His360 (2.76 Å), Arg596 (2.49 Å), Gln363 (1.77 Å), Gln363 (1.99 Å)	electrostatic attractive charge: Arg596 (4.33 Å), $\pi-\pi$ T-shaped: Phe359 (5.19 Å), Trp599 (5.89 Å)
verapamil	−5.1	−38.67	−49.39	−18.22	−28.27	6.15	−1.21	−25.17	43.96	−40.74	conventional H-bond: Thr427 (2.15 Å), carbon H-bond: Thr427 (3.04 Å), Arg596 (2.73 Å), Ala603 (2.41 Å), Glu417 (2.67 Å), Ala603 (2.65 Å), Gly595 (2.88 Å)	salt bridge; electrostatic attractive charge: Glu417 (2.12 Å), π-anion: Glu417 (3.86 Å), $\pi-\pi$ stacked: Trp599 (4.68 Å), Trp599 (3.63 Å), alkyl: Ala426 (3.87 Å), Ala603 (4.48 Å), Ala603 (4.30 Å), Ala606 (3.92 Å), Leu607 (4.81 Å), Leu607 (3.93 Å), Leu420 (5.30 Å), Arg596 (4.46 Å), π-alkyl: Trp599 (3.95 Å), Trp599 (4.79 Å), Ala603 (4.64 Å)
gallic acid	−4.97	−24.08	−23.4	−6.93	53.56	4.12	−2.18	−9.65	−42.83	−24.11	conventional H-bond: Arg596 (2.15 Å), Gln363 (1.88 Å), carbon H-bond: His432 (2.66 Å), $\pi-\pi$ T-shaped: Phe359 (4.88 Å)	electrostatic attractive charge: Arg596 (4.30 Å), $\pi-\pi$ T-shaped: Phe359 (4.88 Å)
vanillic acid	−4.97	−24.2	−11.11	−1.60	32.67	4.12	−3.44	−9.41	−16.03	−16.78	conventional H-bond: Arg596 (2.65 Å), Arg596 (2.10 Å), His600 (1.98 Å), Gln363 (2.09 Å), carbon H-bond: His600 (2.68 Å), π-alkyl: His432 (4.44 Å)	electrostatic attractive charge: Arg596 (3.94 Å), π-alkyl: His432 (4.44 Å)
quercetin	−4.41	−43.93	−32.62	−10.94	−25.6	3.3	−2.08	−9.68	44.25	−38.28	conventional H-bond: His600 (2.20 Å), Ile673 (2.95 Å), carbon H-bond: Leu368 (2.68 Å)	π-donor hydrogen bond: His372 (2.88 Å), $\pi-\pi$ stacked: His367 (4.57 Å), $\pi-\pi$ T-shaped: His372 (5.32 Å), π-alkyl: Leu607 (4.80 Å), Leu607 (5.16 Å)
cinnamic acid	−2.96	−19.93	−7.72	−0.12	65.92	3.66	−1.49	−10.86	−37.42	−25.35	conventional H-bond: Gln303 (2.34 Å), His360 (2.83 Å)	electrostatic attractive charge: Arg596 (4.23 Å), $\pi-\pi$ T-shaped: Phe359 (5.17 Å), Trp599 (5.66 Å)
Voltage-Gated Calcium Ion Channel β2a (VGCC,PDB:1T0J)												
isomangiferin	−8.63	−51.7	−47.04	−17.20	−36.23	5.44	−4.03	−8.15	32.25	−35.3	conventional H-bond: Val60 (3.03 Å), His94 (2.61 Å), His94 (1.58 Å), Ala310 (2.93 Å), carbon H-bond: Ala63 (3.00 Å), Pro224 (1.52 Å), Val223 (2.65 Å), Leu93 (1.31 Å)	π-alkyl: Val60 (5.40 Å), Ala63 (4.95 Å), Pro224 (5.23 Å), Met226 (5.30 Å), Ala63 (3.84 Å), Met226 (5.45 Å), Ala310 (5.46 Å)
iriflophenon glycoside	−6.28	−46.15	−29.63	−9.64	−19.9	10.16	−2.84	−9.19	32.99	−39.62	conventional H-bond: Val95 (2.47 Å), Ala63 (2.49 Å), Phe62 (2.01 Å), Val95 (1.96 Å), (1.90 Å), carbon H-bond: Phe62 (2.80 Å), Pro228 (2.27 Å), (2.40 Å)	π-alkyl: Ala310 (3.88 Å), Leu309 (5.03 Å)
quercetin	−5.44	−37.71	−34.94	−11.95	−14.04	3.66	−2.4	−6.87	14.04	−28.08	conventional H-bond: Phe307 (2.31 Å), Ile303 (2.94 Å), carbon H-bond: Arg311 (2.31 Å)	π-alkyl: Val60 (4.63 Å), Ala63 (3.67 Å), Ala310 (4.43 Å)

https://doi.org/10.1021/acsomega.3c01907
ACS Omega 2023, 8, 26982−27001

Table 2. continued

compounds	docking score	glide energy	dG bind	log pK_i	dG Coulomb	dG covalent	dG H-bond	dG lipo	dG solv GB	dG vdW	H-bond	other bonds
Voltage-Gated Calcium Ion Channel β2a (VGCC,PDB:1T0J)												
mangiferin	−5.23	−39.26	−33.19	−11.19	−36.87	2.26	−3.44	−9.58	47.29	−30.39	conventional H-bond: Phe62 (2.82 Å), Leu93 (2.21 Å), (1.60 Å), (1.75 Å), carbon H-bond: Arg311 (2.34 Å), Leu93 (2.89 Å)	$\pi-\pi$ stacked: Phe307 (5.69 Å), amide-π stacked: Ala61c,O;Phe62 (4.05 Å), π-alkyl: Pro224 (5.12 Å), Arg311 (4.34 Å), Val60 (4.59 Å), Ala63 (4.22 Å), Ala310 (4.75 Å), Arg311 (5.30 Å), Arg311 (4.46 Å)
vanillic acid	−4.14	−18.19	−14.38	−3.02	34.15	3.36	−1.25	−8.89	−19.44	−21.75	conventional H-bond: B:Arg311:H−vanillic acid: O4arg311 (2.71 Å), B:Val316:H−vanillic acid: O2val316 (2.77 Å), vanillic acid: H19−B:Met226: Omet226 (2.84 Å), carbon H-bond: vanillic acid: H16−B:Met226:Omet226 (2.69 Å), vanillic acid: H17−B:Ile306:Oile306 (1.84 Å)	π-alkyl: leu309(4.09 Å)
verapamil	−3.94	−47.44	−46.37	−16.91	−18.55	1.36	−0.62	−15.85	34.96	−46.63	conventional H-bond: Leu93 (2.46 Å), Val223 (2.29 Å), carbon H-bond: Phe92 (2.84 Å), Ala61 (2.86 Å), Ala61 (2.80 Å), Ser225 (2.17 Å), Ser225 (2.58 Å), Gln314 (1.77 Å), Ser225 (2.12 Å)	π-lone pair: Leu93 (2.97 Å), Phe307 (2.86 Å), amide-π stacked: Val64c, O; Arg65 (3.97 Å), Pro224c, O; Ser225 (4.29 Å), alkyl: Ala63 (3.08 Å), Ala63 (4.23 Å), Ala310 (3.66 Å), Met226 (5.04 Å), Val60 (4.19 Å), Val109 (5.29 Å), Val109 (4.45 Å), Val223 (5.40 Å), Arg227 (4.80 Å), π-alkyl: Phe92 (3.63 Å), Phe307 (4.64 Å), Pro224 (5.13 Å), Leu309 (5.44 Å), Val316 (4.44 Å), Val64 (5.08 Å)
gallic acid	−3.85	−20.92	−10.52	−1.34	−4.84	0.32	−2.98	−2.96	11.89	−11.92	conventional H-bond: His398 (3.08)	
caffeic acid	−2.74	−20.38	−19.27	−5.14	−11.43	0.42	−2.21	−7.54	19.21	−16.63	conventional H-bond: His398 (2.12 Å), Leu399 (2.40 Å), carbon H-bond: Ala395 (1.84 Å)	
cinnamic acid	−2.45	−14.99	−10.23	−1.21	25.29	3.8	−0.96	−9.22	−7.44	−20.32	carbon H-bond: Pro228 (2.01 Å), Phe307 (1.93 Å)	π-anion: Phe307 (4.15 Å), π-alkyl: Leu309 (4.62 Å)
Human Myosin Light Chain Kinase-1 (MLCK-1, PDB: 6C6M)												
isomangiferin	−8.41	−43.547	−35.77	−12.31	−32.43	5.3	−4.63	−7.34	29.91	−26.2	conventional H-bond: Lys432 (2.30 Å), Tyr464 (1.85 Å), Tyr471 (2.59 Å), Tyr471 (2.02 Å), Ser486 (2.99 Å), Ser497 (2.02 Å), Ser499 (3.09 Å), Ser497 (2.84 Å), (1.88 Å), Thr430 (2.80 Å), carbon H-bond: Thr430 (3.03 Å), Ser497 (2.68 Å), (2.56 Å), Asp466 (2.61 Å)	π-alkyl: Lys432 (4.02 Å), Lys432 (4.91 Å), Lys432 (3.96 Å)
iriflophenon glycoside	−7.549	−50.881	−0.91	2.83	−110.98	12.84	−5.87	−8.07	137.09	−25.3	conventional H-bond: Trp447 (1.92 Å), Arg456 (2.23 Å), Glu417 (1.99 Å), Glu444 (1.82 Å), Glu436 (2.17 Å), Trp447 (2.87 Å), Val454 (2.25 Å), (1.79 Å), Val445 (1.71 Å), Glu465 (2.32 Å), carbon H-bond: Trp447 (2.91 Å), Trp447 (2.64 Å), Tyr464 (2.81 Å), Glu444 (2.63 Å), Glu417 (2.46 Å), Val454 (2.39 Å)	electrostatic attractive charge: Arg456 (5.58 Å), π-cation: Arg456 (4.31 Å), π-Alkyl: Val463 (4.81 Å)
mangiferin	−6.916	−47.548	−40.48	−14.35	−49.13	7.44	−4.62	−7.75	38.49	−24.58	conventional H-bond: Arg456 (2.04 Å), Arg456 (2.61 Å), Arg456 (2.29 Å), Thr452 (2.09 Å), Val445 (1.60 Å), Val445 (1.70 Å), Glu417 (1.96 Å), (1.53 Å), (1.73 Å), Glu450 (1.67 Å), carbon H-bond: Glu444 (2.70 Å), Glu417 (2.65 Å), Glu417 (2.95 Å), π-donor hydrogen bond: Glu465 (3.02 Å)	
gallic acid	−6.684	−24.759	−10.71	−1.42	−26.28	5.23	−3.19	−6.94	38.98	−18.51	electrostatic attractive charge: Arg456 (3.32 Å), conventional H-bond: Arg456 (2.25	π-alkyl: Ala446 (5.07 Å), Val463 (5.30 Å)

https://doi.org/10.1021/acsomega.3c01907
ACS Omega 2023, 8, 26982−27001

Table 2. continued

compounds	docking score	glide energy	dG bind	log pK_i	dG Coulomb	dG covalent	dG H-bond	dG lipo	dG solv GB	dG vdW	H-bond	other bonds
Voltage-Gated Calcium Ion Channel β2a (VGCC,PDB:1T0J)												
											Å), Glu436 (2.40 Å), Val454 (1.80 Å), Glu444 (1.91 Å), carbon H-bond: Arg456 (3.08 Å), Arg456 (2.56 Å)	
quercetin	−6.39	−37.974	−40.43	−14.33	−42.57	5.48	−2.44	−9.45	34.41	−24.56	conventional H-bond: His470 (1.87 Å), Glu436 (1.61 Å), Trp447 (1.57 Å), π-donor hydrogen bond: Trp447 (2.98 Å)	π-anion: Glu444 (4.99 Å), π-alkyl: Val463 (4.81 Å), Val463 (5.22 Å), Ala446 (4.24 Å), Val463 (5.37 Å)
vanillic acid	−5.176	−22.344	−13.52	−2.64	−20.73	2.8	−1.86	−8.14	31.5	−17.08	conventional H-bond: Glu436 (1.66 Å), carbon H-bond: Arg456 (2.79 Å), Trp447 (2.48 Å), Trp447 (2.62 Å), (2.36 Å), Val454 (2.55 Å)	salt bridge; electrostatic attractive charge: Arg456 (2.10 Å), electrostatic attractive charge: Lys415 (4.90 Å), alkyl: Pro453 (5.43 Å), π-alkyl: Ala446 (5.14 Å)
caffeic acid	−5.16	−29.551	−17.44	−4.34	−6.08	2.14	−1.8	−10.31	28.3	−29.66	conventional H-bond: Trp447 (2.43 Å), Val454 (1.86 Å), Glu436 (1.85 Å), π-donor hydrogen bond: Trp447 (3.14 Å)	electrostatic attractive charge: Arg456 (4.91 Å), π-alkyl: Ala446 (4.10 Å), Val463 (5.35 Å)
cinnamic acid	−2.407	−22.11	−17.26	−4.27	−0.96	0.64	−0.13	−11.11	19.57	−25.25	π-donor hydrogen bond: trp447 (2.82 Å)	salt bridge; electrostatic attractive charge arg: 456 (3.25 Å), π-alkyl: Ala446 (4.12 Å), Val463 (5.46 Å)
verapamil	−2.313	−44.76	−36.37	−12.57	4.36	2.44	−1.48	−14.93	14.51	−40.84	conventional H-bond: Arg480 (2.48 Å), Arg480 (2.44 Å), Glu458 (2.78 Å), carbon H-bond: Arg480 (2.68 Å), Gln457 (2.67 Å), Glu458 (2.62 Å), Ser482 (2.46 Å), Gln457 (2.51 Å), Glu458 (2.74 Å), Asp481 (2.70 Å), Asp481 (2.73 Å), (2.51 Å), Pro453 (2.77 Å), Glu458 (2.65 Å)	alkyl: Val454 (4.29 Å), Arg480 (4.49 Å), π-alkyl: Leu449 (4.37 Å)

[a]dG binding: binding free energy, Log pK_i: logarithmic of inhibition constant (K_i), dG Coulomb: Coulomb binding energy, dG covalent: covalent binding energy, dG H-bond: hydrogen binding energy, dG lipophilic: lipophilic binding energy, dG solv GB: generalized born electrostatic solvation energy, dG vdW: van der Waals forces energy; all these energies contribute to binding free energy (dG binding).

https://doi.org/10.1021/acsomega.3c01907
ACS Omega 2023, 8, 26982−27001

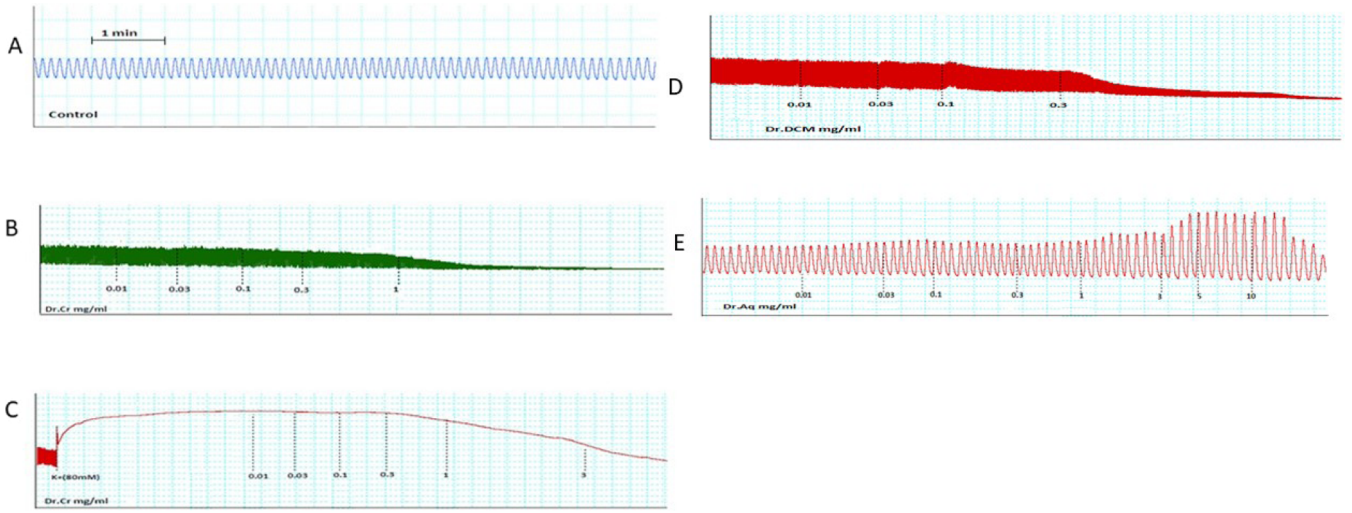

Figure 2. (A) Spontaneously contracting isolated jejunum tissue preparation. Concentration-dependent response of Dr.Cr on (B) spontaneous (C) high-K+ (80 mM)-induced contractions on isolated jejunum tissue. (D) Concentration-dependent response of Dr.DCM on spontaneous contractions on isolated jejunum tissue. (E) Concentration-dependent response of Dr.Aq on spontaneous contractions on isolated jejunum tissue.

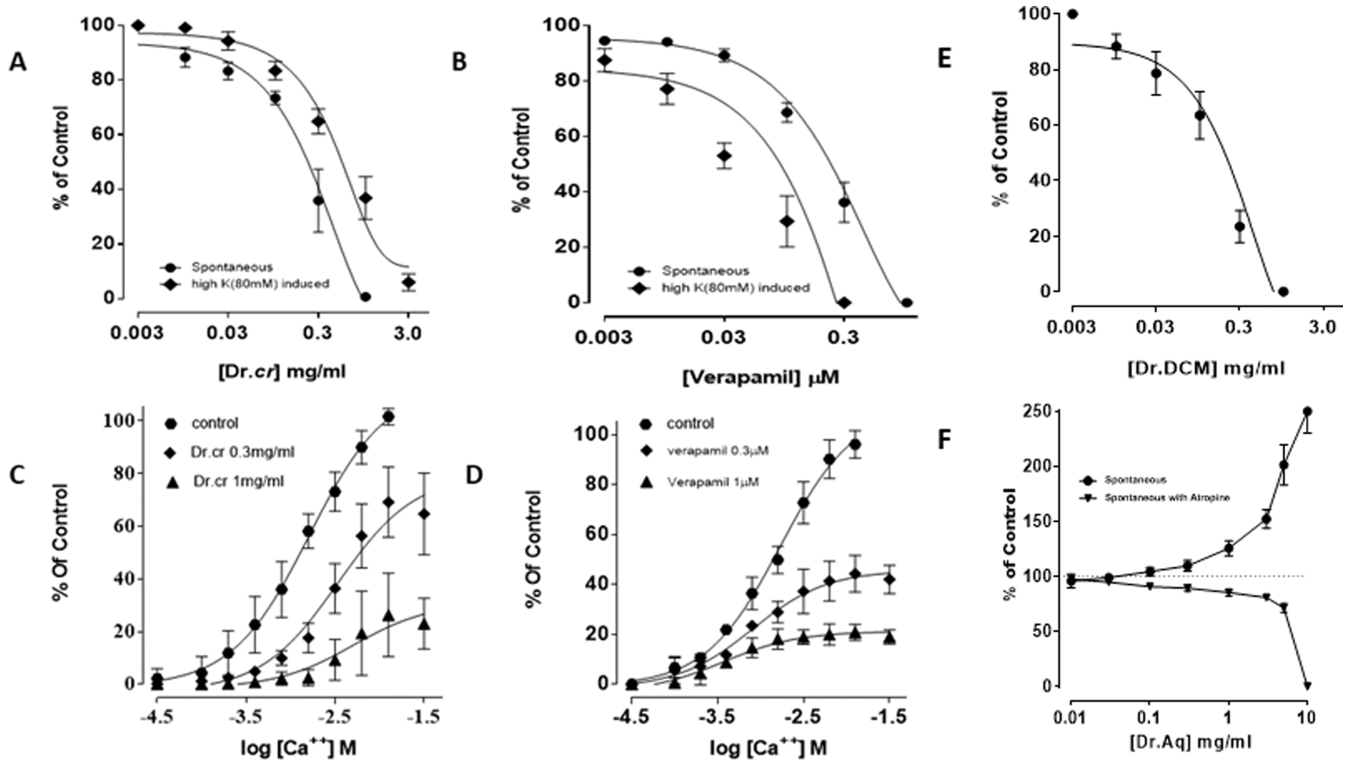

Figure 3. (A) Concentration-dependent response of Dr.Cr on spontaneous and high-K+ (80 mM)-induced contractions in jejunum tissue preparations (N = 5). (B) Concentration-dependent response of verapamil on spontaneous and high-K+ (80 mM)-induced contractions in isolated jejunum tissue preparations (N = 5). (C) Concentration-dependent response of Dr.Cr on the concentration−response curve of calcium (Ca++) in isolated rabbit jejunum tissue preparations (N = 5). (D) Concentration-dependent response of verapamil on the concentration−response curve of calcium (Ca++) in isolated rabbit jejunum tissue preparations (N = 5). (E) Concentration-dependent response of Dr.DCM on spontaneous contractions on isolated jejunum tissue (N = 5). (F) Concentration-dependent response of Dr.Aq on spontaneous contractions and atropine-treated contractions on isolated jejunum tissue (N = 5).

that iriflophenon glycoside, quercetin, and isomangiferin were projected with the least binding energies and referred to as leading bioactive compounds having comparable binding affinities with verapamil (Figure 1 and Table 2).

3.2.2.1. Voltage-Gated Calcium Ion Channel β2a (VGCC, PDB:1T0J). According to what we discovered, isomangiferin (docking score: −8.63 kcal/mol, ΔG binding: −47.04 kcal/mol, pK_i: −17.20 μM) scored 1st for voltage-gated calcium channels and formed conventional H-bonds with Val60 (3.03 Å), His94 (2.61 Å), His94 (1.58 Å), and Ala310 (2.93 Å); carbon H-bonds with Ala63 (3.00 Å), Pro224 (1.52 Å), Val223 (2.65 Å), and Leu93 (1.31 Å); and π-alkyl bonds with Val60 (5.40 Å), Ala63 (4.95 Å), Pro224 (5.23 Å), Met226 (5.30 Å), Ala63 (3.84 Å), Met226 (5.45 Å), and Ala310 (5.46 Å).

https://doi.org/10.1021/acsomega.3c01907
ACS Omega 2023, 8, 26982−27001

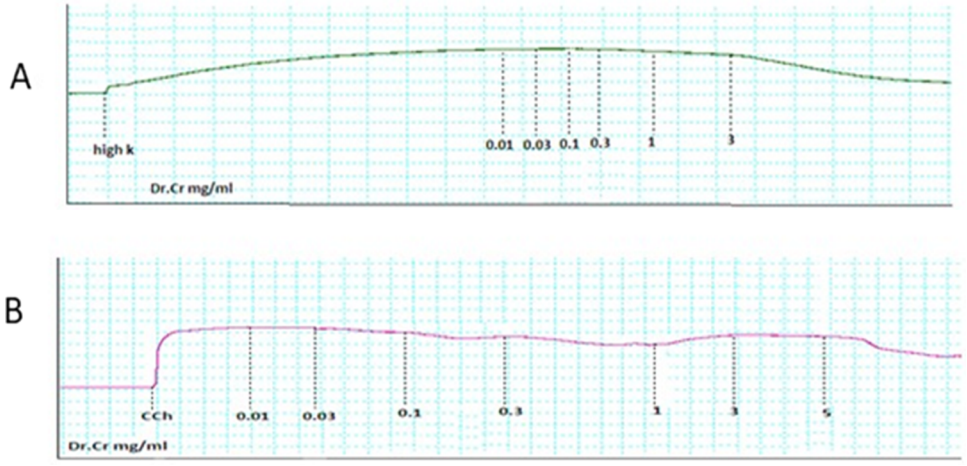

Figure 4. Concentration-dependent response of Dr.Cr on (A) high-K+ (80 mM)-induced and (B) carbachol (1 μM) made contractions in tracheal tissues.

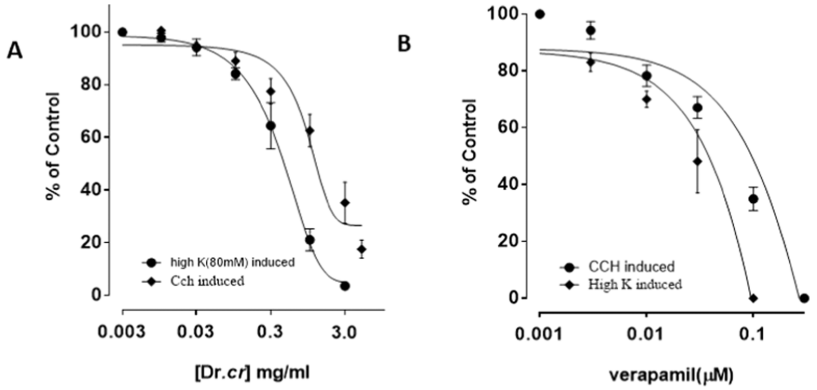

Figure 5. (A) Concentration-dependent response of ethanolic extract Dr.Cr on high-K+ (80 mM)-induced and 1 μM carbachol-induced contractions in isolated tracheal tissues (N = 5). (B) Concentration-dependent response of standard drug verapamil on high-K+ (80 mM)- and 1 μM carbachol-induced contractions in tracheal tissues (N = 5).

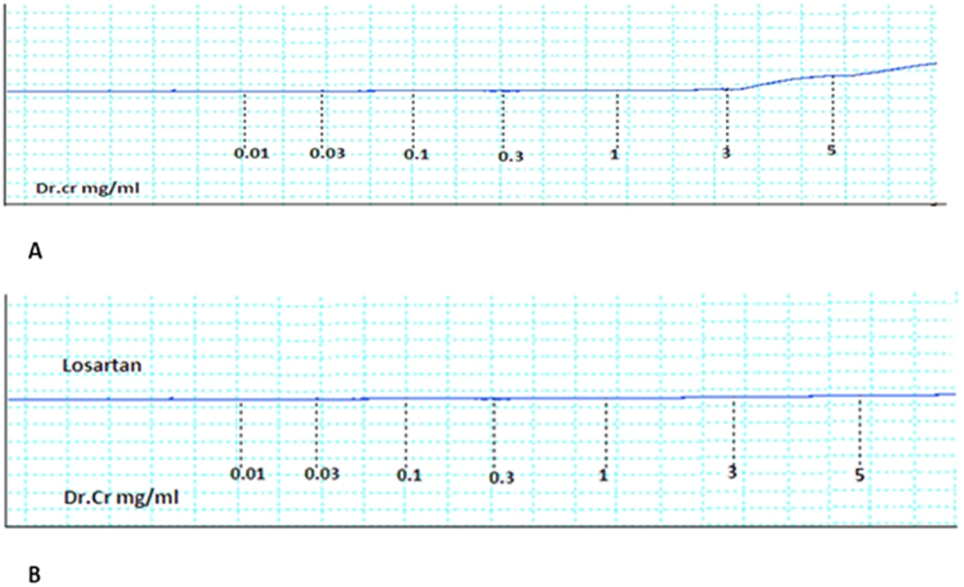

Figure 6. Concentration-dependent response of ethanolic extract Dr.Cr on steadied isolated aortic tissue (a) without losartan and (b) tissue pretreated with losartan.

Iriflophenon glycoside (docking score: −6.28 kcal/mol, ΔG binding: −29.63 kcal/mol, pK_i: −9.46 μM) stood second in its docking score, making conventional H-bonds with Val95 (2.47 Å), Ala63 (2.49 Å), Phe62 (2.01 Å), and Val95 (1.96 Å) and

https://doi.org/10.1021/acsomega.3c01907
ACS Omega 2023, 8, 26982−27001

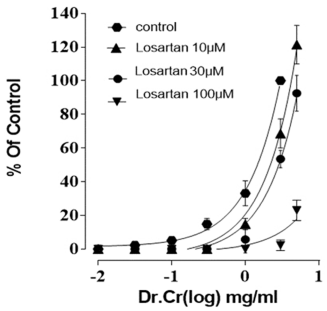

Figure 7. Dose-dependent response of Dr.Cr in isolated aortic rings pretreated with different concentrations of losartan (N = 5).

(1.90 Å); carbon H-bonds with Phe62 (2.80 Å), and Pro228 (2.27 Å), (2.40 Å); and π-alkyl bonds with Ala310 (3.88 Å) and Leu309 (5.03 Å). Quercetin (docking score: −5.44 kcal/mol, ΔG binding: −34.94 kcal/mol, pK_i: −11.95 μM) forms conventional H-bonds with Phe307 (2.31 Å) and Ile303 (2.94 Å); a carbon H-bond with Arg311 (2.31 Å); and π-alkyl bonds with Val60 (4.63 Å), Ala63 (3.67 Å), and Ala310 (4.43 Å). Mangiferin (docking score: −5.23 kcal/mol, ΔG binding: −33.19 kcal/mol, pK_i: −11.19 μM) makes conventional H-bonds with Phe62 (2.82 Å) and Leu93 (2.21 Å), (1.60 Å), and (1.75 Å); carbon H-bonds with Arg311 (2.34 Å) and Leu93 (2.89 Å), π−π stacked with Phe307 (5.69 Å); amide-π stacked with Ala61c,O;Phe62 (4.05 Å); and π-alkyl bonds with Pro224 (5.12 Å), Arg311 (4.34 Å), Val60 (4.59 Å), Ala63 (4.22 Å), Ala310 (4.75 Å), Arg311 (5.30 Å), and Arg311 (4.46 Å). Vanillic acid (docking score: −4.14 kcal/mol, ΔG binding: −14.38 kcal/mol, pK_i: −3.02 μM) forms conventional H-bonds with B:Arg311:H−vanillic acid:O4arg311 (2.71 Å), B:Val316:H−vanillic acid:O2val316 (2.77 Å), and vanillic acid:H19−B:Met226:Omet226 (2.84 Å); carbon H-bonds with vanillic acid:H16−B:Met226:Omet226 (2.69 Å) and vanillic acid:H17−B:Ile306:Oile306 (1.84 Å); and a π-alkyl bond with vanillic acid−B: Leu309leu309 (4.09 Å). Verapamil (docking score: −3.94 kcal/mol, ΔG binding: −46.37 kcal/mol, pK_i: −16.91 μM) forms conventional H-bonds with Leu93 (2.46 Å) and Val223 (2.29 Å); carbon H-bonds with Phe92 (2.84 Å), Ala61 (2.86 Å), Ala61 (2.80 Å), Ser225 (2.17 Å), Ser225 (2.58 Å), Gln314 (1.77 Å), and Ser225 (2.12 Å);π-lone pair with Leu93 (2.97 Å) and Phe307 (2.86 Å); amide-π stacked with Val64c,O;Arg65 (3.97 Å) and Pro224c,O;Ser225 (4.29 Å); alkyl with Ala63 (3.08 Å), Ala63 (4.23 Å), Ala310 (3.66 Å), Met226 (5.04 Å), Val60 (4.19 Å), Val109 (5.29 Å), Val109 (4.45 Å), Val223 (5.40 Å), and Arg227 (4.80 Å); and π-alkyl with Phe92 (3.63 Å), Phe307 (4.64 Å), Pro224 (5.13 Å), Leu309 (5.44 Å), Val316 (4.44 Å), and Val64 (5.08 Å). Gallic acid (docking score: −3.85 kcal/mol, ΔG binding: −10.52 kcal/mol, pK_i: −1.34 μM) makes a conventional H-bond with His398 (3.08). Caffeic acid (docking score: −2.74 kcal/mol, ΔG binding: −19.27 kcal/mol, pK_i: −5.14 μM) forms conventional H-bonds with His398 (2.12 Å) and Leu399 (2.40 Å) and a carbon H-bond with Ala395 (1.84 Å). Cinnamic acid (docking score: −2.45 kcal/mol, ΔG binding: −10.23 kcal/mol, pK_i: −1.21 μM) makes carbon H-bonds with Pro228 (2.01 Å) and Phe307 (1.93 Å); π-anion with Phe307 (4.15 Å); and π-alkyl with Leu309 (4.62 Å).

3.2.2.2. Human Myosin Light Chain Kinase-1 (MLCK-1, PDB: 6C6M). Isomangiferin (docking score: −8.41 kcal/mol, ΔG binding: −35.77 kcal/mol, pK_i: −12.31 μM) makes conventional H-bonds with Lys432 (2.30 Å), Tyr464 (1.85 Å), Tyr471 (2.59 Å), Tyr471 (2.02 Å), Ser486 (2.99 Å), Ser497 (2.02 Å), Ser499 (3.09 Å), Ser497 (2.84 Å), (1.88 Å), and Thr430 (2.80 Å); carbon H-bonds with Thr430 (3.03 Å), Ser497 (2.68 Å), (2.56 Å), and Asp466 (2.61 Å); and π-alkyl with Lys432 (4.02 Å), Lys432 (4.91 Å), and Lys432 (3.96 Å). Iriflophenon glycoside (docking score: −7.549 kcal/mol, ΔG binding: −0.91 kcal/mol, pK_i: −2.83 μM) makes different conventional H-bonds with Trp447 (1.92 Å), Arg456 (2.23 Å), Glu417 (1.99 Å), Glu444 (1.82 Å), Glu436 (2.17 Å), Trp447 (2.87 Å), Val454 (2.25 Å) and (1.79 Å), Val445 (1.71 Å), and Glu465 (2.32 Å); carbon H-bonds with Trp447 (2.91 Å), Trp447 (2.64 Å), Tyr464 (2.81 Å), Glu444 (2.63 Å), Glu417 (2.46 Å), and Val454 (2.39 Å); electrostatic attractive charge with Arg456 (5.58 Å); π-cation with Arg456 (4.31 Å); and π-alkyl with Val463 (4.81 Å). Mangiferin (docking score: −6.916 kcal/mol, ΔG binding: −40.48 kcal/mol, pK_i: −14.35 μM) makes conventional H-bonds with Arg456 (2.04 Å), Arg456 (2.61 Å), Arg456 (2.29 Å), Thr452 (2.09 Å), Val445 (1.60 Å), Val445 (1.70 Å), Glu417 (1.96 Å), (1.53 Å), and (1.73 Å), and Glu450 (1.67 Å); carbon H-bonds with Glu444 (2.70 Å), Glu417 (2.65 Å), and Glu417 (2.95 Å); a π-donor hydrogen bond with Glu465 (3.02 Å). Gallic acid (docking score: −6.684 kcal/mol, ΔG binding: −10.71 kcal/mol, pK_i: −1.42 μM) has electrostatic attractive charge with Arg456 (3.32 Å); conventional H-bonds with Arg456 (2.25 Å), Glu436 (2.40 Å), Val454 (1.80 Å), and Glu444 (1.91 Å); carbon H-bonds with Arg456 (3.08 Å) and Arg456 (2.56 Å); and π-alkyl with Ala446 (5.07 Å) and Val463 (5.30 Å). Quercetin (docking score: −6.39 kcal/mol, ΔG binding: −40.43 kcal/mol, pK_i: −14.33 μM) makes conventional H-bonds with His470 (1.87 Å), Glu436 (1.61 Å), and Trp447 (1.57 Å); π-anion with Glu444 (4.99 Å); π-donor hydrogen bond with Trp447 (2.98 Å); and π-alkyl with Val463 (4.81 Å), Val463 (5.22 Å), Ala446 (4.24 Å), and Val463 (5.37 Å). Vanillic acid (docking score: −5.176 kcal/mol, ΔG binding: −13.52 kcal/mol, pK_i: −2.64 μM) makes a conventional H-bond with Glu436 (1.66 Å); carbon H-bonds with Arg456 (2.79 Å), Trp447 (2.48 Å), Trp447 (2.62 Å), (2.36 Å), and Val454 (2.55 Å); salt bridge and electrostatic attractive charge with Arg456 (2.10 Å);

Table 3. Outcome of Crude Ethanolic Extract *D. ramosa* in Terms of the Percentage of Inflammation Reduced (N = 5; Data Shown as Mean ± SEM)[a]

		% inhibition of paw volume			
groups	dose	0−1 h	0−2 h	0−3 h	0−4 h
group I	NS 0.5 mL				
group II	Aspirin 0.01 g/kg	17.072 + 0.20	21.968 + 0.27	54.864 + 0.29	69.978 + 0.7
group II	Dr.Cr 0.1 g/kg	17.218 + 0.09	19.934 + 0.170	28.6 + 0.27***	36.226 + 0.23***
group IV	Dr.Cr 0.2 g/kg	38.65 + 0.22***	43.648 + 0.377***	50.826 + 0.24*	59.554 + 0.54***

[a]***p < 0.001, **p < 0.01, *p < 0.05 compared with positive control.

https://doi.org/10.1021/acsomega.3c01907
ACS Omega 2023, 8, 26982−27001

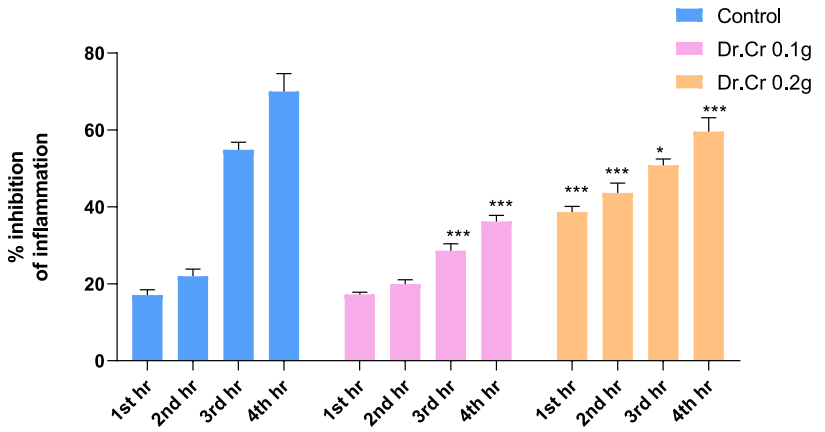

Figure 8. Dr.Cr and aspirin's impact on rat paw edema brought on by carrageenan is measured in terms of the proportion of inhibition of inflammation. Values expressed as mean ± SEM (N = 5). For data analysis, two-way ANOVA with RM testing was used. ***p < 0.001, **p < 0.01, *p < 0.05 compared with positive control.

Table 4. Effect of Ethanolic Plant Extract (Dr.Cr) in Castor Oil-Provoked Diarrhea in Mice (N = 5)

		no. of wet feces			
groups	dose	0−1 h	0−2 h	0−3 h	0−4 h
group I	10 mL/kg	5	8	12	7
group II	5 mg/kg	0	1	1	0
group III	200 mg/kg	2	1	4	0
group IV	400 mg/kg	0	2	3	0

Table 5. Percentage Protection against Castor Oil-Induced Diarrhea by Ethanolic Plant Extract (Dr.Cr)[a,b]

groups	dose	total number of feces	%age protection
group I	10 mL/kg	8 ± 0.50	
group II	5 mg/kg	0.5 ± 0.1***	93.75
group III	200 mg/kg	1.75 ± 0.29**	78.125
group IV	400 mg/kg	1.25 ± 0.26***	84.375

[a]N = 5; data shown as mean ± SEM. [b]***p < 0.001, **p < 0.01, *p < 0.05.

electrostatic attractive charge with Lys415 (4.90 Å); alkyl with Pro453 (5.43 Å); and π-alkyl with Ala446 (5.14 Å). Caffeic acid (docking score: −5.16 kcal/mol, ΔG binding: −17.44 kcal/mol, pK_i: −4.34 μM) forms conventional H-bonds with Trp447 (2.43 Å), Val454 (1.86 Å), and Glu436 (1.85 Å); a π-donor hydrogen bond with Trp447 (3.14 Å); electrostatic attractive charge with Arg456 (4.91 Å); π-alkyl with Ala446 (4.10 Å) and Val463 (5.35 Å). Cinnamic acid (docking score: −2.407 kcal/mol, ΔG binding: −17.26 kcal/mol, pK_i: −4.27 μM) makes a π-donor hydrogen bond with trp447 (2.82 Å); salt bridge and electrostatic attractive charges with 456 (3.25 Å); and π-alkyl with Ala446 (4.12 Å) and Val463 (5.46 Å). Verapamil (docking score: −2.313 kcal/mol, ΔG binding: −36.37 kcal/mol, pK_i: −12.57 μM) makes conventional H-bonds with Arg480 (2.48 Å), Arg480 (2.44 Å), and Glu458 (2.78 Å); carbon H-bonds with Arg480 (2.68 Å), Gln457 (2.67 Å), Glu458 (2.62 Å), Ser482 (2.46 Å), Gln457 (2.51 Å), Glu458 (2.74 Å), Asp481 (2.70 Å), Asp481 (2.73 Å) and (2.51 Å), Pro453 (2.77 Å), and Glu458 (2.65 Å); alkyl with Val454 (4.29 Å) and Arg480 (4.49 Å); and π-alkyl with Leu449 (4.37 Å).

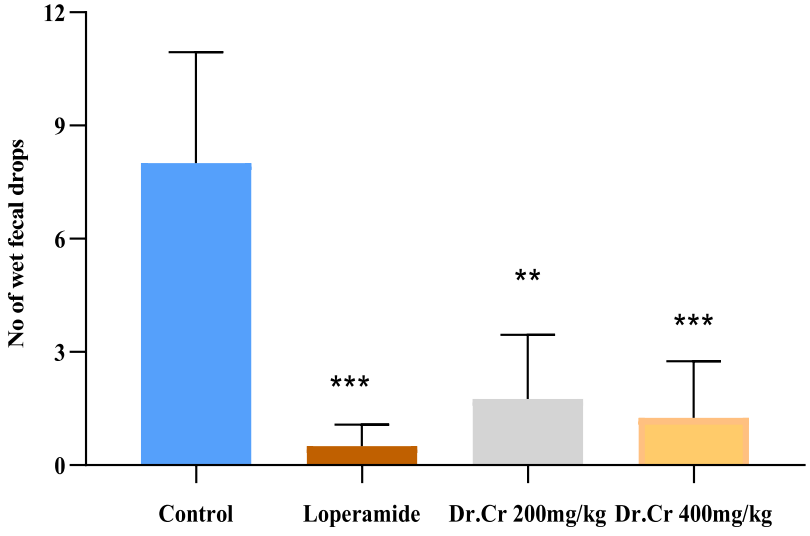

Figure 9. Effect of Dr.Cr on castor oil-induced diarrhea. Values expressed as mean ± SEM (N = 5). For data analysis, the multiple comparison test and standard one-way ANOVA testing were used. ***p < 0.001, **p < 0.01, *p < 0.05 compared with negative control.

https://doi.org/10.1021/acsomega.3c01907
ACS Omega 2023, 8, 26982−27001

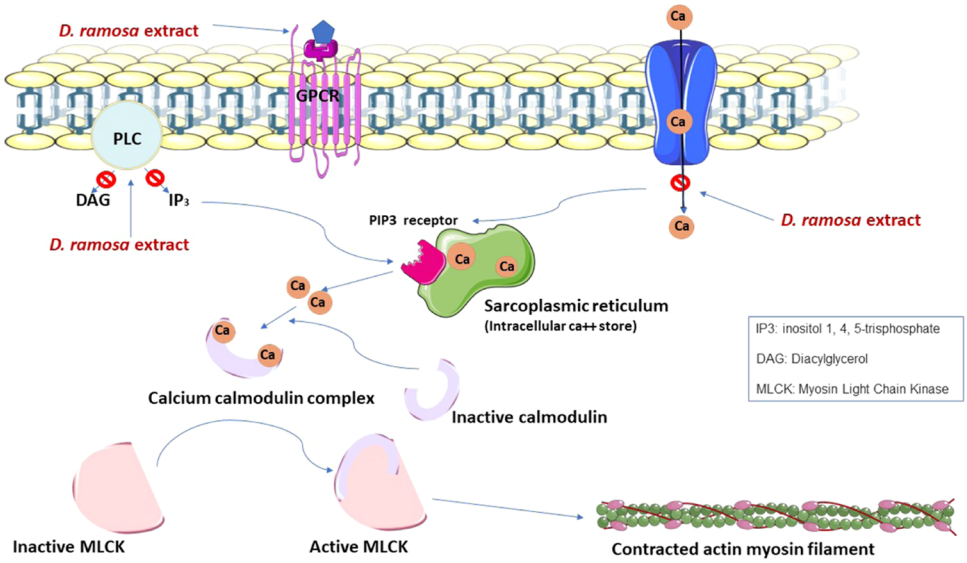

Figure 10. Schematic diagram of the proposed mechanism of *D. ramosa* extracts on the L-type voltage-gated Ca++ channel, M_3 muscarinic receptor, and phosphoinositide phospholipase C (PLC).

3.2.2.3. Human Cyclooxygenase-2 (COX2-PDB:5IkQ). Iriflophenon glycoside (docking score: −9.77 kcal/mol, ΔG binding: −37.8 kcal/mol, pK_i: −13.19 μM) forms conventional H-bonds with Val538 (2.77 Å), Arg377 (2.15 Å), Gly226 (2.24 Å), Asn376 (1.69 Å), Gln375 (1.72 Å), Gln374 (1.97 Å), Asn375 (1.83 Å), and Gly536 (1.92 Å); carbon H-bonds with Pro129 (2.75 Å), Arg377 (2.61 Å), Asn376 (2.67 Å), and Asn376 (3.04 Å); a π-donor hydrogen bond with Asn375 (2.90 Å); and π-cation and π-donor hydrogen bond with Arg376 (4.18 Å). Isomangiferin (docking score: −8.85 kcal/mol, ΔG binding: −38.57 kcal/mol, pK_i: −13.52 μM) makes conventional H-bonds with Arg377 (2.87 Å), Arg377 (2.08 Å), Gln375 (2.81 Å), Gln375 (1.82 Å), Asn375 (1.98 Å), and Ser143 (2.08 Å); carbon H-bonds with Gly226 (2.63 Å), (2.88 Å), and Gln375 (2.59 Å), π-cation with Arg376 (4.97 Å); $\pi-\pi$ T-shaped with Phe142 (4.63 Å); and π-alkyl with Leu145 (5.25 Å). Mangiferin (docking score: −8.03 kcal/mol, ΔG binding: −26.53 kcal/mol, pK_i: −8.29 μM) makes conventional H-bonds with Val228 (2.66 Å), Asn375 (1.76 Å), Arg377 (2.05 Å), Arg377 (3.00 Å), Gln375 (2.46 Å), and Asn376 (1.82 Å) and (1.93 Å); and carbon H-bonds with Gln374 (2.46 Å) and Gln375 (2.79 Å). Quercetin (docking score: −8 kcal/mol, ΔG binding: −44.83 kcal/mol, pK_i: −16.24 μM) makes conventional H-bonds with Arg376 (2.46 Å), Arg376 (2.93 Å), Arg377 (2.26 Å), Val539 (2.81 Å), Asn376 (1.99 Å) and (1.82 Å), Asn375 (2.08 Å), and Gly537 (1.82 Å); and a π-donor hydrogen bond with Asn376 (2.80 Å). Gallic acid (docking score: −6.88 kcal/mol, ΔG binding: −9.38 kcal/mol, pK_i: −0.84 μM) makes conventional H-bonds with Gln242 (2.04 Å), Gln242 (2.57 Å), Arg334 (2.02 Å), Arg334 (1.86 Å), Gly236 (1.85 Å), Gly236 (1.75 Å), and Glu140 (1.95 Å); carbon H-bonds with Ser143 (2.71 Å), Asn144 (2.91 Å), and Leu239 (2.68 Å); and π-lone pair with Glu237 (2.90 Å). Caffeic acid (docking score: −6.05 kcal/mol, ΔG binding: −14.17 kcal/mol, pK_i: −2.92 μM) makes conventional H-bonds with Arg376 (2.13 Å), Arg377 (2.03 Å), Gln375 (1.73 Å), and Asn376 (1.70 Å); and electrostatic attractive charge with Arg376 (3.38 Å). Vanillic acid (docking score: −5.46 kcal/mol, ΔG binding: −14.42 kcal/mol, pK_i: −3.03 μM) makes conventional H-bonds with Arg377 (2.11 Å), Arg377 (2.11 Å), and Gln374 (1.91 Å); a carbon H-bond with Gly226 (2.97 Å); and electrostatic attractive charge with Arg377 (3.47 Å). Verapamil (docking score: −4.31 kcal/mol, ΔG binding: −27.11 kcal/mol, pK_i: −8.54 μM) makes conventional H-bonds with Arg376 (2.78 Å) and Leu224 (2.08 Å); carbon H-bonds with Ser144 (2.32 Å), Gln375 (2.76 Å), Tyr374 (2.75 Å), Gln374 (2.48 Å), Tyr374 (2.56 Å), Gly235 (2.57 Å), Glu236 (2.79 Å), Asp229 (2.68 Å), Glu141 (2.73 Å), and Glu141 (2.70 Å); alkyl with Pro129 (5.04 Å) and Pro127 (4.94 Å), alkyl with Leu238 (4.61 Å); and π-alkyl with Phe142 (4.87 Å) and Phe143 (5.18 Å). Cinnamic acid (docking score: −2.15 kcal/mol, ΔG binding: 0.79 kcal/mol, pK_i: 3.57 μM) makes a conventional H-bond with Asn375-(2.64 Å); a carbon H-bond with Gln374 (2.88 Å); and $\pi-\pi$ T-shaped with Phe143 (4.50 Å).

3.2.2.4. Arachidonate-5-lipoxygenase (ALOX5, PDB: 6n2w). Isomangiferin (docking score: −8.55 kcal/mol, ΔG binding: −47.84 kcal/mol, pK_i: −17.55 μM) makes conventional H-bonds with Thr427 (2.27 Å), Gln363 (1.79 Å), Gln363 (1.65 Å), and Ile673 (2.20 Å) and (1.87 Å) and carbon H-bonds with Leu368 (2.61 Å) and His372 (2.79 Å). Mangiferin (docking score: −8.03 kcal/mol, ΔG binding: −30.3 kcal/mol, pK_i: −9.93 μM) makes conventional H-bonds with His367 (2.19 Å), Thr427 (1.80 Å), Thr427 (2.99 Å), Gln363 (1.88 Å), (1.56 Å), and (1.84 Å), and Glu417 (2.05 Å); a carbon H-bond with (2.57 Å); a carbon H-bond with Gln363 (3.07 Å); $\pi-\sigma$ with Trp599 (2.50 Å); and $\pi-\pi$ T-shaped with Trp599 (5.89 Å) and Trp599 (4.96 Å). Iriflophenon glycoside (docking score: −7.03 kcal/mol, ΔG binding: −32.17 kcal/mol, pK_i: −10.74 μM) makes conventional H-bonds with His367 (2.09 Å), Arg596 (2.77 Å), and Gln363 (1.76 Å), (1.63 Å), and (1.79 Å); carbon H-bonds with Thr427 (3.06 Å), His432 (2.45 Å), Gln363 (2.77 Å), and Gln363 (2.99 Å); a π-cation bond with Arg596 (2.79 Å); $\pi-\pi$ T-shaped with Phe359 (5.33 Å) and Trp599 (5.41 Å); and π-alkyl with Ala603 (5.43 Å) and Ala426 (3.67 Å). Caffeic acid (docking score: −5.19 kcal/mol, ΔG binding: −16.09 kcal/mol, pK_i: −3.76 μM) makes conventional H-bonds with Gln303 (2.19 Å), His360 (2.76 Å), Arg596 (2.49 Å), Gln363 (1.77 Å), and Gln363 (1.99 Å); electrostatic attractive charge

https://doi.org/10.1021/acsomega.3c01907
ACS Omega 2023, 8, 26982−27001

with Arg596 (4.33 Å); and $\pi-\pi$ T-shaped with Phe359 (5.19 Å) and Trp599 (5.89 Å). Verapamil (docking score: −5.1 kcal/mol, ΔG binding: −49.39 kcal/mol, pK_i: −18.22 μM) makes a conventional H-bond with Thr427 (2.15 Å); carbon H-bonds with Thr427 (3.04 Å), Arg596 (2.73 Å), Ala603 (2.41 Å), Glu417 (2.67 Å), Ala603 (2.65 Å), and Gly595 (2.88 Å); salt bridge and electrostatic attractive charge with Glu417 (2.12 Å); π-anion with Glu417 (3.86 Å); $\pi-\pi$ stacked with Trp599 (4.68 Å) and Trp599 (3.63 Å); alkyl with Ala426 (3.87 Å), Ala603 (4.48 Å), Ala603 (4.30 Å), Ala606 (3.92 Å), Leu607 (4.81 Å), Leu607 (3.93 Å), Leu420 (5.30 Å), and Arg596 (4.46 Å); and π-alkyl with Trp599 (3.95 Å), Trp599 (4.79 Å), and Ala603 (4.64 Å). Gallic acid (docking score: −4.97 kcal/mol, ΔG binding: −23.4 kcal/mol, pK_i: −6.93 μM) makes conventional H-bonds with Arg596 (2.15 Å) and Gln363 (1.88 Å); a carbon H-bond with His432 (2.66 Å); $\pi-\pi$ T-shaped with Phe359 (4.88 Å); electrostatic attractive charge with Arg596 (4.30 Å); and $\pi-\pi$ - T-shaped with Phe359 (4.88 Å). Vanillic acid (docking score: −4.97 kcal/mol, ΔG binding: −11.11 kcal/mol, pK_i: −1.60 μM) makes conventional H-bonds with Arg596 (2.65 Å), Arg596 (2.10 Å), His600 (1.98 Å), and Gln363 (2.09 Å); a carbon H-bond with His600 (2.68 Å); π-alkyl with His432 (4.44 Å); electrostatic attractive charge with Arg596 (3.94 Å); and π-alkyl with His432 (4.44 Å). Quercetin (docking score: −4.41 kcal/mol, ΔG binding: −32.62 kcal/mol, pK_i: −10.94 μM) forms conventional H-bonds with His600 (2.20 Å) and Ile673 (2.95 Å); a carbon H-bond with Leu368 (2.68 Å); a π-donor hydrogen bond with His372 (2.88 Å); $\pi-\pi$ stacked with His367 (4.57 Å); $\pi-\pi$ T-shaped with His372 (5.32 Å); and π-alkyl with Leu607 (4.80 Å) and Leu607 (5.16 Å).

Isomangiferin, iriflophenon glycoside, quercetin, mangiferin, and vanillic acid displayed a strong binding affinity for L-type voltage-gated calcium ion channels during molecular docking analysis, and in addition to these, gallic acid, caffeic acid, and cinnamic acid showed an affinity for myosin light chain kinase. All these binding affinities and predicted properties of these bioactive compounds are similar to those of verapamil, a known calcium channel blocker. Therefore, it can be presumed that *D. ramosa* has a powerful antispasmodic effect, which is caused by the significant binding affinity of compounds for their intended protein targets, inhibiting the signal transduction process of smooth muscle contraction. But there is a discrepancy. These predictions invalidate the traditional use and reported in vivo activity of the methanolic extract of *D. ramosa* as a laxative.[44] To address this discrepancy, we have parted the active constituents of the crude ethanolic extract of *D. ramosa* (Dr.Cr) through further polarity-based fractionation into Dr.Aq and Dr.DCM.

3.3. In Vitro Activities. *3.3.1. Response on Rabbit Jejunum Preparations.* For validation of this proposed mechanism of action of *D. ramosa*, all three extracts Dr.Cr, Dr.DCM, and Dr.Aq were evaluated on isolated jejunum tissue preparations. Jejunum is used because of its high reactivity among smooth muscles.[28] An isolated tissue is unaffected by any neurological or hormonal influences and only responds intrinsically, so it is employed for the study of underlying mechanisms.[45] When extracts were added to spontaneously contracting jejunum, diversity in results was found. Dr.Cr resulted in the inhibition of spontaneous contractions and demonstrated spasmolytic action (Figure 2B) in a cumulative dose range of 0.003−1 mg/mL with an EC_{50} value 0.41 mg/mL (95% CI: 0.20−0.85, n = 5) in a manner comparable to verapamil.[46] Dr.DCM also caused suppression of contractions, while Dr.Aq enhanced the contractile response (Figure 2D,E). The spasmogenic effect of Dr.Aq was blocked by atropine (1 μM), thus indicating the presence of some cholinomimetic constituents and supporting its use as a laxative.[47]

There are a number of physiological mediators that regulate the motor tone of the gastrointestinal tract by controlling the movement of Ca++ inside and out of cells.[48] These physiological agents raise cytosolic calcium ion concentrations either by increasing the influx of calcium from the extracellular fluid or by stimulating its release from cytosolic calcium stores.[41] The PLC is stimulated by the M3 muscarinic receptor's activation, and this in turn causes the secondary messenger inositol 1,4,5-trisphosphate (IP3) and diacylglycerol (DAG) to be hydrolyzed from phosphatidylinositol 4,5-bisphosphate. Inositol 1,4,5-trisphosphate receptors (IP3R) on the sarcoplasmic reticulum are stimulated by IP3 to release calcium ions, which raises the level of calcium in the cytosol. The formation of a calcium/calmodulin complex is brought about by the activation of a regulatory protein kinase C (PKC) by DAG and calcium. Myosin light chains (MLCs) are phosphorylated as a result of this calcium/calmodulin combination, activating another myosin light chain kinase (MLCK). Phosphorylated MLCs and actin then form an interaction network to produce a contractile response.[47] The primary cause of smooth muscle spontaneous contraction is a transient rise or drop in free Ca++ in the cytosol. This readily available cytosolic Ca++ interacts with the contractile components of the muscle to generate a transient activation or deactivation of the contractile components, resulting in the elicit of resting membrane potential and the contractile response of smooth muscles (Figure 10).

In order to more thoroughly assess the antispasmodic mode of action of Dr.Cr, rabbit jejunum tissue was exposed to prolonged constriction by addition of high-K+ (80 mM). Studies show that at high concentrations, K+ activates the Ca++ channels (voltage-dependent), causing an invasion of free Ca++ into the cytosol and a significant depolarization of the membrane action potential, which causes a persistent contraction that lasts for a long time.[47] Repolarization results in a relaxation of the smooth muscle.[29] Dr.Cr, when added cumulatively, completely relaxed the high-K+ (80 mM) evoked contractions (Figure 2C) in a tissue organ bath having a concentration of 0.003−3 mg/mL with EC_{50} of 0.76 μM (95% confidence interval: 0.48−1.19, n = 5; Figure 3A), thus preventing the stimulated depolarization. The membrane action potential is repolarized and substances that inhibit smooth muscle contractions caused by high-K+ levels appear to impede Ca++ influx into the cytosol.[47] Verapamil, a common calcium channel blocker that was used as a positive control, demonstrated a comparable response and relaxed both spontaneous and high potassium-induced contractions, with EC_{50} values of 0.34 μM (95% CI: 0.22−0.51, n = 5) and 0.04 μM (95% CI: 0.02−0.10, n = 5), respectively (Figure 3B). For confirmation of the calcium channel-blocking response of Dr.Cr, CRCs of calcium were constructed in the absence and presence of extract. All Ca++ channel blockers have the trait of blocking calcium's sluggish entry, and this effect can be reversed by adding Ca++.[49] Pretreating with the extract Dr.Cr caused calcium CRCs to be suppressed at doses of 0.3 and 1 mg/mL with a rightward parallel shift on jejunum tissue preparation, comparable to that of verapamil at doses of 0.1 and 0.3 μM.[50] These results were compared with the common

https://doi.org/10.1021/acsomega.3c01907
ACS Omega 2023, 8, 26982−27001

calcium channel blocker verapamil, which caused complete suppression of CRCs at doses of 0.3 and 1 μM compared to Dr.Cr (Figure 3C,D). This outcome suggests the existence of Ca++ channel blockers in Dr.Cr, since they are helpful in cases when the gut is overactive.[49] Wahid et al. reported the strong affinity of quercetin with PLC.[47] Antispasmodic agents disrupt this pathway, and they are used to treat overactive gastrointestinal ailments.[29,51] Numerous investigations have revealed that the Ca++ antagonistic effect of medicinal herbs is the primary cause of their mode of action.[50] Multiple diseases can be cured through the interactions between bioactive substances and their target proteins.[52]

3.3.2. Response on the Trachea. The potential bronchodilator properties of *D. ramosa* were investigated, as it has the presence of flavonoids, and besides their antispasmodic properties, flavonoids are also known to play a role as bronchodilators.[53−55] Capasso et al.[37] studied the bronchodilator effect of quercetin on rat tracheal tissues. Djelili et al.[38] reported that quercetin and rutin had a bronchodilator effect on isolated human bronchus tissues. Chang et al.[56] reported the antiasthmatic activity of quercetin and rutin. Ko et al.[57] studied the broncho-relaxant effect of quercetin on KCl (30 mM), and carbachol (0.2 μM)-induced spastic contraction on isolated guinea pig tracheal tissue preparations. To explore the mechanism of relaxation, investigations of Dr.Cr were conducted in isolated rabbit tracheal preparations that had already been precontracted with CCh (1 μM) and high-K+ (80 mM).[58] Dr.Cr inhibited high-K+ (80 mM)-induced contraction in rabbit tracheal preparation (Figure 4) in a dose-dependent manner with a corresponding EC_{50} of 0.6194 mg/mL (95% CI: 0.388 to 0.988, n = 5). The response of Dr.Cr on CCh-induced contraction was insignificant, since it did not totally relax the contraction caused by 1 μM CCh until 10 mg/mL (Figure 5A). So, it confirmed the speculations that the extract contained some cholinomimetic and calcium channel blocker constituents,[47] and CCB was a prominent mechanism for the bronchodilator effect.[59] Partial relaxation of CCh-induced contractions showed that Dr.Cr had some muscarinic M3 receptor activity, which is masked at higher doses by some other bioactive agonist compounds, as depicted by the spasmogenic effect of Dr.Aq at the jejunum (Figure 2E). Comparatively, verapamil, a common Ca++ channel antagonist, reduced high-K+ (80 mM), and CCh (1 μM) provoked contractions with corresponding EC_{50} values of 0.063 μM/mL (95% CI: 0.02−0.17, n = 5) and 0.09 μM/mL (95% CI: 0.063−0.14, n = 5; Figure 5B). Given that they are intended to be tracheal relaxants, CCBs are also known to be useful as a cough remedy.[60]

3.3.3. Effect on the Aorta. Moreover, the smooth muscle relaxant effect of Dr.Cr was confirmed on isolated aortic rings where it caused a contractile reaction on stable aortic tissue preparation (Figure 6A), potentially as a result of activation of one or more types of receptors on the aorta. This contractile response of Dr.Cr decreases when tissue is pretreated with losartan (Figure 6B). Dose−response curves of Dr.Cr after pretreatment with increasing concentrations of losartan are made, and it is shown in Figure 7 that by increasing the concentration of losartan, dose−response curves are shifted toward the right by suppression of contractions at initial doses of Dr.Cr, which are concluded to be mediated through activation of angiotensin II receptors.[31]

3.4. In Vivo Activities. *3.4.1. Effect on Carrageenan-Induced Rat Paw Edema.* The presence of flavonoids in *D. ramosa* suggests the anti-inflammatory effect of plants, as studies have shown the relation of the anti-inflammatory effect of plants with the presence of flavonoids.[18] Dr.Cr significantly reduced the inflammation by inhibiting edema in the paws of rats at dosages of 0.1 and 0.2 g/kg in treatment groups compared to the control group. Carrageenan causes edema to develop in two stages. During the first hour following carrageenan exposure, histamines, serotonins, prostaglandins, and cytoplasmic enzymes are released from neighboring cells of wounded tissue. After the first hour, the second phase begins, and it is characterized by a rise in prostaglandin secretion and the release of leukotrienes and kinins from the inflammatory area.[61,62] The suppression of edema following pretreatment with Dr.Cr (0.1 g/kg; I/P), at time intervals of the 1st, 2nd, 3rd, and 4th hours, was measured to be 17.218, 19.934, 28.6, and 36.226%, respectively. In contrast, pretreatment with Dr.Cr (0.2 g/kg, I/P) led to percentages of 38.65, 43.648, 50.826, and 59.554% at respective intervals of the 1st, 2nd, 3rd, and 4th hours, respectively, while standard aspirin therapy (0.01 g/kg; I/P) resulted in 17.072, 21.968, 54.864, and 69.978% suppression of inflammation, respectively (Table 3 and Figure 8). Dr.Cr substantially reduced the edema in the second phase and proposed that it works by inhibiting the formation of cyclooxygenase. This result is equivalent to that of nonsteroidal anti-inflammatory medications. These results are also validated by the results of our docking studies, which showed strong interaction of bioactive compounds from ethanolic extract of *D. ramosa* like iriflophenon glycoside, isomangiferin, mangiferin, and different polyphenolic compounds quercetin, gallic acid, caffeic acid, vanillic acid, and cinnamic acid with the human cyclooxygenase-2 enzyme, suggesting the role of these compounds in anti-inflammatory activity.

3.4.2. Effect on Diarrhea Brought on by Castor Oil. Diarrhea is described as the abnormal passing of soft stools as a result of problems with the colon's ability to carry water and electrolytes. Castor oil alters colonic water and electrolyte transport, which results in diarrhea and increases peristaltic motions.[63] Dr.Cr caused a significant decline in the number of wet drops of feces in mice (Table 4). Group I (positive control group) receiving normal saline (NS) at 10 mL/kg dose showed 8 ± 0.50 wet drops of feces. Group II (negative control) receiving loperamide at 5 mg/kg dose showed 0.5 ± 0.1 fecal drops. Groups III and IV receiving extract at 200 and 400 mg/kg doses showed 1.75 ± 0.29 and 1.25 ± 0.26 fecal drops, respectively (Table 5 and Figure 9). As shown in (Table 5) both 200 and 400 mg/kg doses of ethanolic crude extract were found to produce a decrease in the frequency of defecation and diarrheal stools in castor oil-treated mice groups in 4 h observations in comparison to the negative control (normal saline) group. There was significant postponement in the commencement of diarrhea at a dose of 400 mg/kg comparable to loperamide. This dose-dependent increase in protection from diarrhea plus delay in onset of diarrhea at a high dose (84.38% at dose 400 mg/kg) is comparable to loperamide (93.75% at 10 mg/kg dose; Table 5). Loperamide has a propensity to interfere with the calcium-mediated signaling system, hence regulating intestinal tone.[64] Thus, in vivo results showed that extract reduces intestinal tone experiments by blocking the calcium channel. These results are supported by in vitro and in silico studies (Figure 10).

https://doi.org/10.1021/acsomega.3c01907
ACS Omega 2023, 8, 26982−27001

4. CONCLUSIONS

The prospective compounds like quercetin, mangiferin, and isomangiferin are promising bioactive compounds of *Dryopteris ramose*, which showed a strong binding affinity to L-type voltage-gated Ca++ channels, human myosin light chain kinase, Cox2, and arachidonate-5-lipoxygenase during computational studies and during validation of these proposed effects through biological experiments. The hydroethanolic extract (Dr.Cr) of *D. ramosa* (Linn.) exhibited spasmolytic, spasmogenic, bronchodilator, and vasoconstrictive activities through different mechanisms. The spasmolytic and bronchodilator activities are mediated through blockage of Ca++ channels, spasmogenic activity through activation of muscarinic receptors, and vasoconstrictive activity may be due to the presence of angiotensin II agonistic compounds. Also, it has anti-inflammatory activity, so it may be helpful in treating asthma as well as diarrhea by controlling the contractile effect via calcium-mediated signaling.

AUTHOR INFORMATION

Corresponding Authors

Fatima Saqib − *Department of Pharmacology, Bahauddin Zakariya University, Multan 60000, Pakistan*; orcid.org/0000-0001-6242-7147; Email: fatima.saqib@bzu.edu.pk

Lorena Dima − *Faculty of Medicine, Transilvania University of Brasov, Brasov 500036, Romania*; Email: lorenadima@yahoo.com

Authors

Iram Iqbal − *Department of Pharmacology, Bahauddin Zakariya University, Multan 60000, Pakistan*

Muhammad Farhaj Latif − *Department of Pharmacology, Bahauddin Zakariya University, Multan 60000, Pakistan*

Hamna Shahzad − *Department of Biochemistry, Bahauddin Zakariya University, Multan 60000, Pakistan*

Bayan Sajer − *Department of Biological Sciences, College of Science, King Abdulaziz University, Jeddah 80200, Saudi Arabia*

Rosana Manea − *Faculty of Medicine, Transilvania University of Brasov, Brasov 500036, Romania*

Ciprian Pojala − *Faculty of Medicine, Transilvania University of Brasov, Brasov 500036, Romania*

Radu Necula − *Faculty of Medicine, Transilvania University of Brasov, Brasov 500036, Romania*

Complete contact information is available at: https://pubs.acs.org/10.1021/acsomega.3c01907

Author Contributions

F.S. and I.I.: conceptualization; M.F.L. and H.S.: methodology; L.D., R.M., C.P., and R.N.: validation; I.I.: formal analysis; I.I., B.S., and L.D.: data curation; F.S., B.S., I.I., M.F.L., and H.S.: writing—original draft preparation; and L.D., R.M., C.P., and R.N.: writing—review and editing. All authors have read and agreed to the published version of the manuscript.

Funding

This research received no external funding.

Notes

The authors declare no competing financial interest.

REFERENCES

(1) Pirintsos, S.; Panagiotopoulos, A.; Bariotakis, M.; Daskalakis, V.; Lionis, C.; Sourvinos, G.; Karakasiliotis, I.; Kampa, M.; Castanas, E. From Traditional Ethnopharmacology to Modern Natural Drug Discovery: A Methodology Discussion and Specific Examples. *Molecules* **2022**, *27*, No. 4060.

(2) Heinrich, M. New medicines based on traditional knowledge: Indigenous and intellectual property rights from an ethnopharmacological perspective. *Ethnopharmacology* **2015**, 75−86.

(3) Heinrich, M.; Gibbons, S. Ethnopharmacology in drug discovery: an analysis of its role and potential contribution. *J. Pharm. Pharmacol.* **2010**, *53*, 425−432. From NLM.

(4) Wahid, M.; Ali, A.; Saqib, F.; Aleem, A.; Bibi, S.; Afzal, K.; Ali, A.; Baig, A.; Khan, S. A.; Bin Asad, M. H. H. Pharmacological exploration of traditional plants for the treatment of neurodegenerative disorders. *Phytother. Res.* **2020**, *34*, 3089−3112.

(5) Hon, K.-L.; Ki Fung, C.; KC Leung, A.; Ngan-Ho Leung, T.; KK Ng, D. Complementary and alternative medicine for childhood asthma: an overview of evidence and patents. *Recent Pat. Inflammation Allergy Drug Discovery* **2015**, *9*, 66−79.

(6) Wen, M.-C.; Wei, C.-H.; Hu, Z.-Q.; Srivastava, K.; Ko, J.; Xi, S.-T.; Mu, D.-Z.; Du, J.-B.; Li, G.-H.; Wallenstein, S. Efficacy and tolerability of antiasthma herbal medicine intervention in adult patients with moderate-severe allergic asthma. *J. Allergy Clin. Immunol.* **2005**, *116*, 517−524.

(7) Hameed, S.; Hans, S.; Nandan, S.; Fatima, Z. Mechanistic insights into the antimycobacterial action of unani formulation, Qurs Sartan Kafoori. *J. Tradit. Complementary Med.* **2022**, *12*, 162−171.

(8) Hamayun, M. Ethnobotanical profile of Utror and Gabral valleys, district Swat, Pakistan. *Ethnobotanical leaflets* **2005**, *2005*, 9.

(9) Shinwari, Z. K.; Qaiser, M. Efforts on conservation and sustainable use of medicinal plants of Pakistan. *Pak. J. Bot.* **2011**, *43*, 5−10.

(10) Tariq, A.; Adnan, M.; AbdElsalam, N. M.; Fouad, H.; Hussain, K.; Ullah, R.; Ullah, A. Richness and cover of nontimber economic plants along altitude in temperate Himalayan forest-use types. *Sci. World J.* **2014**, *2014*, No. 748490. From NLM.

(11) Benjamin, A.; Manickam, V. *Medicinal pteridophytes from the Western Ghats*, 2007.

(12) Alam, F.; Khan, S. H. A.; Asad, M. Phytochemical, antimicrobial, antioxidant and enzyme inhibitory potential of medicinal plant *Dryopteris ramosa* (Hope) C. Chr. *BMC Complementary Med. Ther.* **2021**, *21*, No. 197. From NLM.

(13) Arshad, M.; Ahmad, M. Medico-botanical investigation of medicinally important plants from Galliyat areas, NWFP (Pakistan). *Ethnobotanical Leaflets* **2004**, *2004*, 6.

(14) (a) Sabeen, M.; Ahmad, S. S. Exploring the folk medicinal flora of Abbotabad city, Pakistan. *Ethnobotanical Leaflets* **2009**, *2009*, 1. (b) Adnan, M.; Begum, S.; Latif, A.; Tareen, A. M.; Lee, L. Medicinal plants and their uses in selected temperate zones of Pakistani Hindukush-Himalaya. *J. Med. Plants Res.* **2012**, *6*, 4113−4127.

(15) Abbasi, A. M.; Khan, M. A.; Shah, M. H.; Shah, M. M.; Pervez, A.; Ahmad, M. Ethnobotanical appraisal and cultural values of medicinally important wild edible vegetables of Lesser Himalayas-Pakistan. *J. Ethnobiol. Ethnomed.* **2013**, *9*, 66. From NLM.

(16) Ahmad, K. S.; Qureshi, R.; Hameed, M.; Ahmad, F.; Nawaz, T. Conservation assessment and medicinal importance of some plants resources from Sharda, Neelum Valley, Azad Jammu and Kashmir, Pakistan. *Int. J. Agric. Biol.* **2012**, *14*, 997−1000.

(17) Ahmad, K. S.; Habib, S. Indigenous knowledge of some medicinal plants of Himalaya region, Dawarian village, Neelum valley, Azad Jammu and Kashmir, Pakistan. *Univers. J. Plant Sci.* **2014**, *2*, 40−47.

(18) Mir, S. A.; Mishra, A. K.; Reshi, Z. A.; Sharma, M. P. Preliminary phytochemical screening of some pteridophytes from district Shopian (J & K). *Int. J. Pharm. Pharm. Sci.* **2013**, *5*, 632−637.

(19) Ishaque, M.; Bibi, Y.; Qayyum, A.; Iriti, M. Isolation and Structural Confirmation of Xanthone Isomers from *Dryopteris ramosa* (Hope) C. Chr. and Their In Vitro Antioxidant Mechanism. *Arabian J. Sci. Eng.* **2021**, *46*, 5327−5337.

https://doi.org/10.1021/acsomega.3c01907
ACS Omega 2023, 8, 26982−27001

(20) Bashir, S.; Janbaz, K. H.; Jabeen, Q.; Gilani, A. H. Studies on spasmogenic and spasmolytic activities of Calendula officinalis flowers. *Phytother. Res.* **2006**, *20*, 906−910. From NLM.
(21) Abdur Rahman, H. M.; Bashir, S.; Gilani, A. H. Calcium channel blocking activity in Desmostachya bipinnata (L.) explains its use in gut and airways disorders. *Phytother. Res.* **2013**, *27*, 678−684. From NLM.
(22) Council, N. *National Institutes of Health Guide for the Care and Use of Laboratory Animals*; The National Academies Press: Washington, DC, 2011.
(23) Baloch, R.; Uzair, M.; Chauhdary, B. Phytochemical analysis, antioxidant and cytotoxic activities of *Dryopteris ramosa*. *Biomed. Res.* **2019**, *30*, 764−769.
(24) Ishaque, M.; Bibi, Y.; Ayoubi, S. A.; Masood, S.; Nisa, S.; Qayyum, A. Iriflophenone-3-C-β-d Glucopyranoside from *Dryopteris ramosa* (Hope) C. Chr. with Promising Future as Natural Antibiotic for Gastrointestinal Tract Infections. *Antibiotics* **2021**, *10*, 1128.
(25) Daina, A.; Michielin, O.; Zoete, V. SwissADME: a free web tool to evaluate pharmacokinetics, drug-likeness and medicinal chemistry friendliness of small molecules. *Sci. Rep.* **2017**, *7*, No. 42717.
(26) Pires, D. E. V.; Blundell, T. L.; Ascher, D. B. pkCSM: predicting small-molecule pharmacokinetic and toxicity properties using graph-based signatures. *J. Med. Chem.* **2015**, *58*, 4066−4072.
(27) Sirous, H.; Chemi, G.; Campiani, G.; Brogi, S. An integrated in silico screening strategy for identifying promising disruptors of p53-MDM2 interaction. *Comput. Biol. Chem.* **2019**, *83*, No. 107105.
(28) Saqib, F.; Usman, F.; Malik, S.; Bano, N.; Ur-Rahman, N.; Riaz, M.; Vlaic, R. A. M.; Mureşan, C. C. Antidiarrheal and Cardio-Depressant Effects of Himalaiella heteromalla (D. Don) Raab-Straube: In Vitro, In Vivo, and In Silico Studies. *Plants* **2022**, *11*, No. 78.
(29) Saqib, F.; Janbaz, K. H. Rationalizing ethnopharmacological uses of Alternanthera sessilis: A folk medicinal plant of Pakistan to manage diarrhea, asthma and hypertension. *J. Ethnopharmacol.* **2016**, *182*, 110−121.
(30) Rehman, S.; Imran, M. An ethno-botanical review of seeds of Cucumis sativa (Maghz-e-tukhme khiyarain) from Unani Medicine and its Pharmacological Updates. *Int. J. Adv. Pharm. Med. Bioallied Sci.* **2021**, *9*, 31−36.
(31) Janbaz, K. H.; Zaeem, A. M.; Saqib, F.; Imran, I.; Zia-Ul-Haq, M.; Abid, R. M.; Jaar, H.Z.E.; Moga, M. Scientific Basis for Use of Pyrus pashia Buch.-Ham. ex D. Don. Fruit in Gastrointestinal, Respiratory and Cardiovascular Ailments. *PLoS One* **2015**, *10*, No. e0118605.
(32) Gilani, A. H.; Bashir, S.; Janbaz, K. H.; Khan, A. Pharmacological basis for the use of Fumaria indica in constipation and diarrhea. *J. Ethnopharmacol.* **2005**, *96*, 585−589. From NLM.
(33) García, X.; Cartas-Heredia, L.; Lorenzana-Jímenez, M.; Gijón, E. Vasoconstrictor effect of Cissus sicyoides on guinea-pig aortic rings. *Gen. Pharmacol.* **1997**, *29*, 457−462.
(34) Ratheesh, M.; Helen, A. Anti-inflammatory activity of Ruta graveolens Linn on carrageenan induced paw edema in wistar male rats. *Afr. J. Biotechnol.* **2007**, *6*, 1209−12011.
(35) Zarei, M.; Mohammadi, S.; Komaki, A. Antinociceptive activity of Inula britannica L. and patuletin: in vivo and possible mechanisms studies. *J. Ethnopharmacol.* **2018**, *219*, 351−358.
(36) Balarastaghi, S.; Delirrad, M.; Jafari, A.; Majidi, M.; Sadeghi, M.; Zare-Zardini, H.; Karimi, G.; Ghorani-Azam, A. Potential benefits versus hazards of herbal therapy during pregnancy; a systematic review of available literature. *Phytother. Res.* **2022**, *36*, 824−841.
(37) Capasso, R.; Aviello, G.; Romano, B.; Atorino, G.; Pagano, E.; Borrelli, F. Inhibitory effect of quercetin on rat trachea contractility in vitro. *J. Pharm. Pharmacol.* **2009**, *61*, 115−119.
(38) Djelili, H.; Arrar, L.; Naline, E.; Devillier, P. Relaxant Effects of Quercetin and Rutin on Human Isolated Bronchus. *Chin. Med.* **2012**, *03*, 94−100.
(39) *Release, S. 1: QikProp*; Schrödinger, LLC: New York, NY, 2020.
(40) Waszkowycz, B.; Clark, D. E.; Gancia, E. Outstanding challenges in protein−ligand docking and structure-based virtual screening. *Wiley Interdiscip. Rev.: Comput. Mol. Sci.* **2011**, *1*, 229−259.
(41) Wahid, M.; Saqib, F.; Qamar, M.; Ziora, Z. M. Antispasmodic activity of the ethanol extract of Citrullus lanatus seeds: Justifying ethnomedicinal use in Pakistan to treat asthma and diarrhea. *J. Ethnopharmacol.* **2022**, *295*, No. 115314.
(42) Ventura-Martinez, R.; Angeles-Lopez, G. E.; Gonzalez-Trujano, M. E.; Carrasco, O. F.; Deciga-Campos, M. Study of Antispasmodic and Antidiarrheal Activities of Tagetes lucida (Mexican Tarragon) in Experimental Models and Its Mechanism of Action. *J. Evidence-Based Complementary Altern. Med.* **2020**, *2020*, No. 7140642. From NLM.
(43) Amira, S.; Rotondo, A.; Mulè, F. Relaxant effects of flavonoids on the mouse isolated stomach: structure-activity relationships. *Eur. J. Pharmacol.* **2008**, *599*, 126−130. From NLM.
(44) Nazir, S.; Khan, H.; Khan, S. A.; Alam, W.; Ghaffar, R.; Khan, S. H. A.; Daglia, M. In vivo acute toxicity, laxative and antiulcer effect of the extract of Dryopteris Ramose. *Cell. Mol. Biol.* **2021**, *67*, 9−16.
(45) Ajay, M.; Chai, H. J.; Mustafa, A. M.; Gilani, A. H.; Mustafa, M. R. Mechanisms of the anti-hypertensive effect of Hibiscus sabdariffa L. calyces. *J. Ethnopharmacol.* **2007**, *109*, 388−393. From NLM.
(46) Yasin, M.; Hussain Janbaz, K.; Imran, I.; Gilani, A. U.; Bashir, S. Pharmacological studies on the antispasmodic, bronchodilator and anti-platelet activities of Abies webbiana. *Phytother. Res.* **2014**, *28*, 1182−1187. From NLM.
(47) Wahid, M.; Saqib, F.; Ahmedah, H. T.; Gavris, C. M.; De Feo, V.; Hogea, M.; Moga, M.; Chicea, R. Cucumis sativus L. seeds ameliorate muscular spasm-induced gastrointestinal and respiratory disorders by simultaneously inhibiting calcium mediated signaling pathway. *Pharmaceuticals* **2021**, *14*, 1197.
(48) Sharkey, K.; MacNaughton, W. Pharmacotherapy of Gastric Acidity, Peptic Ulcers, and Gastroesophageal Reflux Disease. In *Goodman and Gilman's: The Pharmacological Basis of Therapeutics*; Mcgraw Hill, 2018; Vol. *13*.
(49) Wahid, M.; Saqib, F. Scientific basis for medicinal use of Citrullus lanatus (Thunb.) in diarrhea and asthma: In vitro, in vivo and in silico studies. *Phytomedicine* **2022**, *98*, No. 153978.
(50) Saqib, F.; Janbaz, K. H. Ethnopharmacological basis for folkloric claims of Anagallis arvensis Linn.(Scarlet Pimpernel) as prokinetic, spasmolytic and hypotensive in province of Punjab, Pakistan. *J. Ethnopharmacol.* **2021**, *267*, No. 113634.
(51) Bin-Jumah, M.; Alwakeel, S. S.; Moga, M.; Buvnariu, L.; Bigiu, N.; Zia-Ul-Haq, M. Application of Carotenoids in Cosmetics. In *Carotenoids: Structure and Function in the Human Body*; Springer, 2021; pp 747−756.
(52) Zia-Ul-Haq, M. Past, Present and Future of Carotenoids Research. In *Carotenoids: Structure and Function in the Human Body*; Springer, 2021; pp 827−854.
(53) Saqib, F.; Janbaz, K. H.; Latif, M. F.; Gilani, A. H.; Bashir, S. Ethnopharmacological studies on antispasmodic, bronchodilator and antiplatelet aggregation activities of Blepharis edulis Pers. *Asian J. Nat. Appl. Sci.* **2012**, *1*, 33−45.
(54) Khalid, A.; Zaheer ul, H.; Ghayur, M. N.; Feroz, F.; Atta ur, R.; Gilani, A. H.; Choudhary, M. I. Cholinesterase inhibitory and spasmolytic potential of steroidal alkaloids. *J. Steroid Biochem. Mol. Biol.* **2004**, *92*, 477−484. From NLM.
(55) Ghayur, M. N.; Khan, H.; Gilani, A. H. Antispasmodic, bronchodilator and vasodilator activities of (+)-catechin, a naturally occurring flavonoid. *Arch. Pharmacal Res.* **2007**, *30*, 970−975. From NLM.
(56) Jung, C. H.; Ji, Y. L.; Chul, H. C.; Chang, J. K. Anti-asthmatic action of quercetin and rutin in conscious guinea-pigs challenged with aerosolized ovalbumin. *Arch. Pharmacal Res.* **2007**, *30*, 1599−1607.
(57) Ko, W.-C.; Liu, P.-Y.; Chen, J.-L.; Leu, I.-J.; Shih, C.-M. Relaxant Effects of Flavonoids in Isolated Guinea Pig Trachea and Their Structure-Activity Relationships. *Planta Med.* **2003**, *69*, 1086−1090.
(58) Janbaz, K. H.; Jan, A.; Qadir, M. I.; Gilani, A. H. Spasmolytic, bronchodilator and vasorelaxant activity of methanolic extract of

https://doi.org/10.1021/acsomega.3c01907
ACS Omega 2023, 8, 26982−27001

Tephrosia purpurea. *Acta Pol. Pharm.* **2013**, *70*, 261−269. From NLM.
(59) Ahmed, T. Calcium antagonists: potential for asthma therapy. *Choices Respir Manage* **1992**, *22*, 41−43.
(60) Kamei, J.; Kasuya, Y. Antitussive effects of Ca2+ channel antagonists. *Eur. J. Pharmacol.* **1992**, *212*, 61−66. From NLM.
(61) Kumar, V.; Kaithwas, G.; Anwar, F.; Rahman, M.; Patel, D. K.; Singh, Y.; Verma, A. Effect of variable doses of Paederia foetida L. combat against experimentally-induced systemic and topical inflammation in Wistar rats. *Curr. Bioact. Compd.* **2018**, *14*, 70−79.
(62) Muller, J. A. I.; Moslaves, I. S. B.; Oliveira, E. J. T.; Portugal, L. C.; Oliveira, R. J.; Mortari, M. R.; Toffoli-Kadri, M. C. Pro-inflammatory response induced by the venom of Parachartergus fraternus wasp. *Toxicon* **2021**, *190*, 11−19.
(63) Agbor, G. A.; Longo, F.; Makong, E. A.; Tarkang, P. A. Evaluation of the antidiarrheal and antioxidant properties of Justicia hypocrateriformis. *Pharm. Biol.* **2014**, *52*, 1128−1133. From NLM.
(64) Crowe, A.; Wong, P. Potential roles of P-gp and calcium channels in loperamide and diphenoxylate transport. *Toxicol. Appl. Pharmacol.* **2003**, *193*, 127−137.

https://doi.org/10.1021/acsomega.3c01907
ACS Omega 2023, 8, 26982−27001